

NOAA Technical Memorandum NWS NHC 38

**THE NATIONAL HURRICANE CENTER RISK ANALYSIS PROGRAM
(HURISK)**

Prepared by:

Charles J. Neumann
Science Applications International Corporation

Contract No. 50-DGNC-6-00209

National Hurricane Center
Coral Gables, Florida
November 1987
Reprinted with corrections August 1991

UNITED STATES
DEPARTMENT OF COMMERCE
Robert A. Moshbacher, Secretary

National Oceanic and Atmospheric Administration
John A. Knauss
Under Secretary and Administrator

National Weather Service
Elbert W. Friday
Assistant Administrator



TABLE OF CONTENTS

	INTRODUCTION AND PURPOSE.....	1
	SCOPE.....	2
3.0	THE DATA BASE.....	3
3.1	<u>COMPUTER DATA FILES</u>	3
3.2	<u>DATA QUALITY</u>	3
4.0	FREQUENTLY USED TERMINOLOGY.....	3
4.1	<u>SCAN CIRCLES</u>	3
4.2	<u>CLOSEST-POINT-OF-APPROACH (CPA)</u>	4
	BRIEF DESCRIPTION OF PROGRAM OUTPUT.....	4
6.0	DESCRIPTION OF INDIVIDUAL CHARTS.....	5
6.1	<u>CHART 1</u>	5
6.1.1	Columns 1 and 2.....	7
6.1.2	Columns 3 through 6.....	7
6.1.3	Column 7.....	7
6.1.4	Column 8, 9 and 10.....	8
6.2	<u>CHART 2</u>	8
6.2.1	Chart Description.....	8
6.2.2	Technical Discussion (Wind Asymmetries).....	8
6.3	<u>CHART 3</u>	11
6.4	<u>CHART 4</u>	11
6.4.1	Chart Description.....	11
6.4.2	Technical Discussion.....	13
6.4.2.1	<u>A statistical pitfall</u>	13
6.4.2.2	<u>Applicability of Poisson distribution</u>	13
6.5	<u>CHART 5</u>	14
6.6	<u>CHART 6</u>	14
6.7	<u>CHART 7</u>	17
6.7.1	Chart Description.....	17
6.7.2	Technical Discussion.....	17
6.7.2.1	<u>Line of best fit</u>	17
6.7.2.2	<u>A mathematical problem</u>	17
6.7.2.3	<u>The role of RMW</u>	19
6.8	<u>CHART 8</u>	19
6.8.1	Chart Description.....	19
6.8.2	Technical Discussion.....	19
6.8.2.1	<u>Choice of Weibull distribution</u>	19
6.8.2.2	<u>Adequacy of fit</u>	21
6.9	<u>CHART 9</u>	21
6.9.1	Chart Description.....	21
6.9.1.1	<u>Wind return periods for site</u>	21
6.9.1.2	<u>Areal wind return periods</u>	21
6.9.1.3	<u>N-year events</u>	23
6.9.1.4	Further applications of Chart 9.....	23
6.9.2	Technical Discussion.....	24
6.9.2.1	<u>Areal return periods (mathematical derivation)</u>	24
6.9.2.2	<u>Maximum possible storm intensity</u>	25
6.9.2.3	<u>A simplified procedure</u>	26

6.9.2.4	<u>Summary of Chart 9 restrictions</u>	27
6.10	<u>CHART 10</u>	27
6.10.1	Chart Description.....	27
6.10.2	Technical Discussion (Estimated Mean).....	29
6.11	<u>CHART 11</u>	29
6.12	<u>CHART 12</u>	29
6.12.1	Chart Description.....	29
6.12.2	Technical Discussion.....	32
6.12.2.1	<u>Integration of Gamma distribution</u>	32
6.12.2.2	<u>Parameter estimation</u>	32
6.13	<u>CHART 13</u>	32
6.13.1	Chart Description.....	32
6.13.2	Technical Discussion.....	34
6.13.2.1	<u>Application of "t-test"</u>	34
6.14	<u>CHART 14</u>	34
6.14.1	Chart Description.....	34
6.14.2	Technical Discussion.....	36
6.15	<u>CHART 15</u>	36
6.16	<u>CHART 16</u>	36
6.17	<u>CHART 17</u>	38
6.18	<u>CHART 18</u>	38
7.0	<u>SUMMARY</u>	38
7.1	<u>IMPORTANT ISSUES</u>	38
7.2	<u>REQUEST FOR USER COMMENTS</u>	39
A	<u>APPENDIX</u>	40
A.1	<u>PURPOSE</u>	40
A.2	<u>BACKGROUND</u>	40
A.3	<u>THE DISTANCE FUNCTION</u>	42
A.4	<u>THE WIND FUNCTION</u>	42
A.4.1	Maximum Likelihood Estimators.....	42
A.4.2	Random Selection from Weibull Distribution.....	43
A.4.3	Adjustment of R_f in Eq. (A5).....	43
A.5	<u>RADIUS OF MAXIMUM WIND (RMW)</u>	43
A.5.1	RMW Methodology used in HURISK.....	44
A.5.1.1	<u>Pressure-wind relationships</u>	44
A.5.1.2	<u>RMW/maximum wind/latitude relationships</u>	45
A.5.1.3	<u>Standard deviation of RMW</u>	46
A.6	<u>LOG-NORMAL DISTRIBUTIONS OF RMW</u>	46
A.6.1	Truncation of Distributions.....	48
A.7	<u>A PROGRAM BRANCH</u>	48
A.7.1	Procedure if Storm Distance from Site \leq RMW.....	48
A.7.2	Procedure if Storm Distance from Site $>$ RMW.....	50
A.8	<u>HORIZONTAL (STANDARDIZED) WIND PROFILES</u>	50
A.8.1	Application of Profiles.....	50
A.9	<u>FRICITIONAL EFFECTS</u>	50
A.9.1	Over-water to Over-land Wind Reduction.....	50
A.9.2	Inland Wind Reduction.....	52
A.10	<u>SIMULATION PERIOD</u>	52
A.11	<u>ADDITIONAL "TUNING" OF SYSTEM</u>	52
A.12	<u>CONFIDENCE FACTORS</u>	52
	<u>REFERENCES</u>	54

THE NATIONAL HURRICANE CENTER RISK ANALYSIS PROGRAM (HURISK)

Charles J. Neumann
Science Applications International Corporation¹

ABSTRACT

The National Hurricane Center has developed a computerized model for assessing the long-term vulnerability of coastal areas to tropical cyclone events. Program output, essentially graphical, is in the form of 18 charts and diagrams. These charts depict tropical cyclone tracks, motion, intensity and wind return periods for any coastal or near-coastal site over the Atlantic tropical cyclone basin. For input, the program accesses current NHC files of historical tropical cyclone data. Program output can therefore be updated as the need arises.

This publication is intended primarily as a user's manual, describing the utility of the various charts. However, minor technical discussion, as warranted by individual chart complexity, is also given. A major technical discussion, contained in an Appendix, describes derivation of tropical cyclone return periods using a Monte-Carlo simulation procedure.

1.0 INTRODUCTION AND PURPOSE

The primary responsibility of the National Hurricane Center (NHC) is detection, tracking and forecasting of tropical cyclones. As an adjunct duty, the NHC assumes the role of a tropical cyclone information center and its expertise is routinely sought on matters pertaining to these storms. Requests for information come from many sources and cover a variety of topics. Frequently, these relate to tropical cyclone climatology and range from simple factual inquiries on some historical event to more in-depth issues on, for example, tropical cyclone risk analysis.

In addition to these external information requests, the NHC requires rapid access to tropical cyclone information in connection with many of its internal functions. The latter would include routine day-to-day forecasting operations and the Center's extensive commitment to the storm-surge program (Jarvinen and Damiano, 1985). Accordingly, the NHC maintains rather extensive computer and non-computer files relating to historical tropical cyclone events and associated environmental parameters.

Computer programs to facilitate access to these data have been evolving at the NHC for many years. One of the early motivations for rapid computer access to and processing of tropical cyclone data was in connection with the NASA Space Program in the late 1960's (Hope and Neumann, 1968, Neumann, 1969). Early attempts to profitably use these data in operational tropical cyclone prediction led to the development of the NHC analog forecast model, HURRAN (HURRICANE ANALOGS), described by Hope and Neumann, (1970) and the CLIPER (CLIMatology and PERSistence) fore-

¹ Prepared for the National Hurricane Center, Coral Gables, FL 33146:
Contract No. 50-DGNC-6-00209

cast model, described by Neumann (1972). These programs, which predict tropical cyclone motion based on past events, are dependent on the NHC maintaining an adequate computer file of historical storm information. The current computer algorithm for processing the data base has evolved to the point where it satisfactorily addresses most user requests as well as NHC internal needs for tropical cyclone related climatic data. Although the program will be continually updated as the need arises, it has become reasonably stable such that a user manual is feasible and, indeed, highly desirable. This document satisfies this need. An earlier, but very abbreviated, description of the program output was given by Neumann (1985).

2.0 SCOPE

The report is intended as a user's rather than a programmer's guide and, as such, will avoid topics related to the latter unless they promote better user understanding of program output. Programming issues are treated separately in NHC internal documents. The computer source code, written originally in the FORTRAN IV language but with recent FORTRAN 77 extensions, is quite large, consisting of 81 sub-programs exclusive of plotting routines. In the interest of keeping the document within some reasonable page size, it would have been impractical to include an appendix of program code as is sometimes done in manuals of this type. Program output is essentially graphical and, although supplementary printout is generated, this is typically not needed by users. The program, referred to hereinafter as HURISK (HUrricane RISK), was specifically designed to be graphically self-sufficient.

The intent of the report is threefold: (a) to provide users with rather basic descriptions of the various charts and graphs produced by HURISK, (b) to cite some chart applications and, (c) to provide details on some of the technical issues involved. Minor technical issues are discussed in the body of the text with the major technical issue -- a description of the storm simulation procedure -- being reserved for the Appendix. A list of references provide additional documentation to some of the more complex technical issues. The style of presentation assumes that the user has at least some basic understanding of tropical cyclones. Also, a background in probability theory is desirable for proper understanding of some of the technical issues although every attempt has been made to simplify these as much as possible.

The program is typically initiated at the NHC through a remote computer terminal linked to the NOAA NAS 9000 series mainframe computer system in Suitland, MD. However, the source code was written with eventual intent of activating the program on less powerful, even personal computer systems. This latter goal did lead to some trade-offs in program structure and output.

Similarly, graphical output is currently obtained through the NOAA FR80 graphics facility in Suitland, MD. However, as with the source code, the graphics output code was designed for eventual local production at NHC on less sophisticated plotting systems. Indeed, all graphics included herein were produced on a small, desk-top, x-y plotter available to the author, rather than on the FR80 system.

3.0 THE DATA BASE

Important to an understanding of the program output, is an understanding of the tropical cyclone data base which provide program input. Indeed, technical design of the program, particularly the risk analysis portion, was strongly influenced by the available data. In general, the complexity of the program was kept commensurate with the quality of the data base.

COMPUTER DATA FILES

The computer data base begins with the year 1886. It is updated annually and, when corrections are brought to the attention of the NHC, modifications to the file are made. The file contains, among other entries, storm positions, maximum sustained winds and central pressures² at 6-hourly intervals. Over the 102-year period, 1886 through 1987, a total of 852 Atlantic tropical cyclones are documented. A complete description of the data set is given by Jarvinen, et al. (1984). Additional characteristics and limitations of the data are discussed by Neumann et al. (1987)³. Although records on tropical cyclones do exist prior to the year 1886, these are too fragmented and uncertain to be included in the computer file. The NHC also maintains similar files for other tropical cyclone basins for which it has operational or research responsibility and the computer algorithm described herein has been activated on these other basins, as well.

DATA QUALITY

In general, the reliability of the data gradually improves from the beginning of the data-set in 1886 to the present. Tropical cyclones typically occur over remote marine areas and the opportunity to directly measure such parameters as surface wind and pressure seldom exists; much must be inferred from indirect evidence. This is particularly true in the pre-satellite era (prior to mid-1960's) and even more true in the pre-aircraft reconnaissance era (prior to mid-1940's). Users of these data should be aware of data imperfections, uncertainties and limitations and should consult the two references cited in the preceding paragraph for additional guidance.

4.0 FREQUENTLY USED TERMINOLOGY

4.1 SCAN-CIRCLES

Tropical cyclones are a relatively rare event. As noted earlier, a total of 852 tropical cyclones of various intensities have been documented over the Atlantic basin over the 102-year period, 1886-1987. This is approximately 8 or 9 storms per year, on the average. Since these storms can occur anywhere over the basin, the chance of a given

² Pressure data are extremely fragmented for the early years.

³ It is highly recommended that HURISK users have access to this document for background on Atlantic tropical cyclones.

site experiencing a direct hit in a given year is very small. For this reason, any analysis of tropical cyclones for a given site must also consider storms which pass at some distance from the site. This distance should be large enough to ensure an adequate sample of storms, yet small enough to preserve the climatological integrity of the site under consideration. Experience has shown that a distance of 75 nautical miles (139 kilometers) is a reasonable compromise. In practice, a circle of that radius (referred to subsequently as a scan-circle or scan-radius) is positioned on the site and all storms passing through this scan-circle are included in the analysis. Over the Atlantic basin, this distance typically encompasses between 40 and 80 storms per 100 years and this is sufficient for all program options. A radius of 150 n.mi. (278 km.) is used in the return-period computations (see Appendix).

4.2 CLOSEST-POINT-OF-APPROACH (CPA)

Along with the use of the term, "scan-circle", as described above, reference will frequently be made to "CPA". This is the minimum distance from the storm center to the site based on hourly storm positions. These were interpolated from 6-hourly storm positions contained on the computer history file using methodology suggested by Akima (1970).

5.0 BRIEF DESCRIPTION OF PROGRAM OUTPUT

With all options activated, HURISK produces a total of 18 charts and graphs, describing various aspects of tropical cyclone climatology and behavior for any number of sites. For each site, these charts are:

- Chart 01: A list of tropical cyclones which have passed within a specified distance from the site over some specified period of record.
- Chart 02: A Mercator map showing the tracks of the above storms.
- Chart 03: Same as Chart 02 except for hurricanes only
- Chart 04: A chronological depiction of storm occurrence for the site over the period of record.
- Chart 05: A depiction of intra-seasonal variations in storm frequency.
- Chart 06: A depiction of storm heading distribution as storms pass near the site.
- Chart 07: Chart showing the number of tropical cyclones passing within lesser scan-radii from the site with fitted mathematical function.
- Chart 08: Histogram of observed maximum winds for all storms affecting the site together with fitted Weibull distribution.
- Chart 09: Return periods of various intensity tropical cyclones at site and within various distances from site.

- Chart 10: Chart depicting probability of multiple tropical storm and hurricane events over various consecutive-year intervals.
- Chart 11: Same as Chart 10 except for hurricanes only.
- Chart 12: Gamma distribution of tropical cyclone translational speeds in vicinity of site.
- Chart 13: Same as Chart 12 except for hurricanes only.
- Chart 14: Geographical distribution of storm frequency in vicinity of site.
- Chart 15: Same as Chart 14 except for hurricanes only.
- Chart 16: Geographical variation of tropical cyclone motion characteristics in vicinity of site.
- Chart 17: Same as Chart 16 except for hurricanes only.
- Chart 18: Overlay to enhance appearance of charts when using overhead projector for display.

6.0 DESCRIPTION OF INDIVIDUAL CHARTS

In this section, each of the charts introduced above will be described. The site example used here is San Juan, Puerto Rico (Latitude/Longitude = 18.4N/66.0W)⁴. This Caribbean site, along with Miami, Florida and a few other locations have rather lengthy and reliable tropical cyclone records. These were extensively used in program development to verify some of the climatological projections made by the HURISK program.

Reference will occasionally be made to supplementary program output. This output can also be made available to users in the form of standard computer print-out. However, except in special circumstances, this supplementary output is not required for full understanding of the graphical output.

The actual size and arrangements of most of the charts are a function of the data. Also, some of the charts are designed to adjust their dimensions depending on the period of record and thus will change slightly from one year to the next. If a severe hurricane strikes a particular area, the user may wish to rerun the series to note the effect, if any, on the climatological expectancies for the site.

6.1 CHART 1

Chart 1 (Fig. 1) gives a list of tropical cyclones which had winds of at least tropical storm strength (≥ 34 knots) while passing within 75 n.mi. of San Juan over the 102-year period, 1886 through 1987. In practice,

⁴ In HURISK, latitudes and longitudes are specified in degrees and tenths of degrees.

TROPICAL CYCLONES (1886-1987) PASSING WITHIN 75 N.MI. OF SAN JUAN

STORM INDEX NUMBER	STORM NAME	YEAR	MONTH	DAY (GMT)	STORM NUMBER FOR YEAR	MAXIMUM WIND (KTS)	CLOSEST POINT OF APPROACH (CPA) NMI	STORM HEADING (DEGS) AT CPA	STORM FORWARD SPEED AT CPA (KTS)
1	NOT NAMED	1887	OCT	10	11	78	71	270	13.2
2	NOT NAMED	1891	AUG	20	3	83	4	302	9.1
3	NOT NAMED	1891	OCT	3	7	45	19	270	10.5
4	NOT NAMED	1893	AUG	17	3	90	7	296	11.2
5	NOT NAMED	1898	SEP	1	2	103	32	305	10.5
6	NOT NAMED	1898	SEP	22	5	40	20	297	9.4
7	NOT NAMED	1898	OCT	28	9	50	49	270	10.5
8	NOT NAMED	1899	AUG	8	2	100	16	298	10.8
9	NOT NAMED	1900	AUG	31	1	45	32	282	10.7
10	NOT NAMED	1900	OCT	25	7	35	51	314	9.3
11	NOT NAMED	1901	JUL	7	3	68	49	307	8.4
12	NOT NAMED	1901	SEP	12	6	40	23	273	17.1
13	NOT NAMED	1901	OCT	9	9	35	11	304	13.4
14	NOT NAMED	1903	JUL	20	1	35	6	298	12.9
15	NOT NAMED	1908	SEP	10	4	68	59	283	17.5
16	NOT NAMED	1908	SEP	26	6	50	56	269	14.3
17	NOT NAMED	1910	SEP	7	2	85	42	275	10.5
18	NOT NAMED	1916	JUL	13	2	45	42	307	5.9
19	NOT NAMED	1916	AUG	22	5	73	1	270	11.4
20	NOT NAMED	1916	OCT	9	12	87	71	353	10.1
21	NOT NAMED	1924	AUG	19	2	40	36	317	12.4
22	NOT NAMED	1926	JUL	23	1	68	48	303	14.8
23	NOT NAMED	1928	SEP	13	4	140	9	298	12.9
24	NOT NAMED	1930	SEP	2	2	102	53	285	7.9
25	NOT NAMED	1931	AUG	17	4	35	7	312	10.3
26	NOT NAMED	1931	SEP	11	6	72	11	275	12.4
27	NOT NAMED	1932	SEP	27	7	90	6	270	13.8
28	NOT NAMED	1933	JUL	15	3	35	55	270	12.4
29	NOT NAMED	1933	JUL	28	5	83M	56	293	13.3
30	NOT NAMED	1933	SEP	28	16	40	36	266	16.2
31	NOT NAMED	1938	AUG	8	1	52	16	273	17.1
32	NOT NAMED	1940	AUG	5	3	40	61	289	15.9
33	NOT NAMED	1942	NOV	5	10	37	21	304	35.6
34	NOT NAMED	1947	OCT	17	9	61	63	299	14.1
35	NOT NAMED	1949	SEP	3	4	45	42	307	17.3
36	BAKER	1950	AUG	23	2	34	33	292	10.3
37	HILDA	1955	SEP	12	8	46	64	285	11.7
38	BETSY	1956	AUG	12	3	80	8	305	17.4
39	EDITH	1958	AUG	19	6	35	63	270	29.6
40	ELDISE	1975	SEP	16	5	38	51	281	10.6
41	FREDERIC	1979	SEP	4	6	45	7	270	9.5
42	GERT	1981	SEP	8	7	48	9	308	18.0
43	KLAUS	1984	NOV	7	12	45	21	041	7.3

9

CHART

Fig. 1. List of storms

this distance can be varied but, as discussed earlier, a 75 n.mi. radius scan-circle is preferred and indeed, required, if a risk analysis is to be performed. It can be noted that a total of 43 storms, of various intensity, have passed through this circular area over the period of record. Actually, the site location is adjusted slightly to account for asymmetries in the wind rotating about the storm center. This adjustment is discussed in Section 6.2.2. Chart 1 is subdivided into 10 columns.

6.1.1 Columns 1 and 2

Column 1 gives a chronologically assigned index number which is used internally by the program. Column 2 gives the storm name. These names are the official storm names used by the National Hurricane Center. The practice of formally naming storms began in the year 1950 and the term "not named" is used prior to that date; however, unnamed storms are occasionally encountered after 1950. Additional background on naming of tropical cyclones is given by Neumann et al. (1987).

6.1.2 Columns 3 through 6

Columns 3, 4, 5 and 6 specifically identify the storm as to its date-time of passage closest to the site and is in agreement with storm documentation in the above cited reference. Supplementary non-graphical program output further specifies the time of day when the storm was closest to the site.

6.1.3 Column 7

Column 7 refers to the maximum wind near the storm center. Maximum winds referred to in the HURISK program are technically defined as the maximum near-surface wind averaged over a time duration of 60-seconds. However, the opportunity or the ability to measure winds with the accuracy implied by this definition, seldom exists. Also, shorter duration gusts (and lulls) in the wind are apt to be considerably higher (or lower) than the 60-second sustained wind. This topic and the methodology to estimate shorter period gusts is discussed by Simiu and Scanlan (1978).

The wind data given in column 7 refer to the time of storm passage closest to the site -- referred to as closest point of approach or CPA in columns 8, 9 and 10. These are the winds which are later used by the program (along with other parameters) to compute wind return periods at the site itself.

While winds at CPA are used for the computation of return periods, winds elsewhere in the scan-circle are used for other purposes in the program. Charts 3, 11, and 13, for example, refer to storms which were of hurricane strength at some point within the scan circle, not necessarily at CPA. To avoid what might appear to be a program inconsistency, such situations are flagged with an asterisk (*) adjacent to the wind in column 7. In this example, it can be noted that storm number 29 is so flagged. This storm was classified as a tropical storm at the closest-point-of-approach to San Juan but became a hurricane to the northwest of the city, just prior to exiting the scan-circle.

Two wind parameters have been discussed in the preceding two paragraphs; (1) maximum intensity inside the scan-circle and (2) storm intensity at CPA. An additional wind parameter could be the average wind while the storm was within the scan-circle. Although not further used in program computations, these average winds are given in supplementary program output.

6.1.4 Column 8, 9 and 10

Column 8 gives, in units of nautical miles, the closest point of approach (CPA) of the storm to the site (actually, to an adjusted site -- see Section 6.2.2) while columns 9 and 10, respectively, give storm translational speed in units of nautical miles per hour (knots) and storm heading⁵. Tropical cyclone headings are traditionally specified as the direction towards which the storm is moving. These speeds and directions are computed by averaging over the available storm positions immediately before and after CPA. The master data file gives storm positions every 6 hours and these are interpolated to hourly positions for use in the program. Additional tabular data relating to storms passing through the scan circle are given in supplementary program output.

6.2 CHART 2

6.2.1 Chart Description

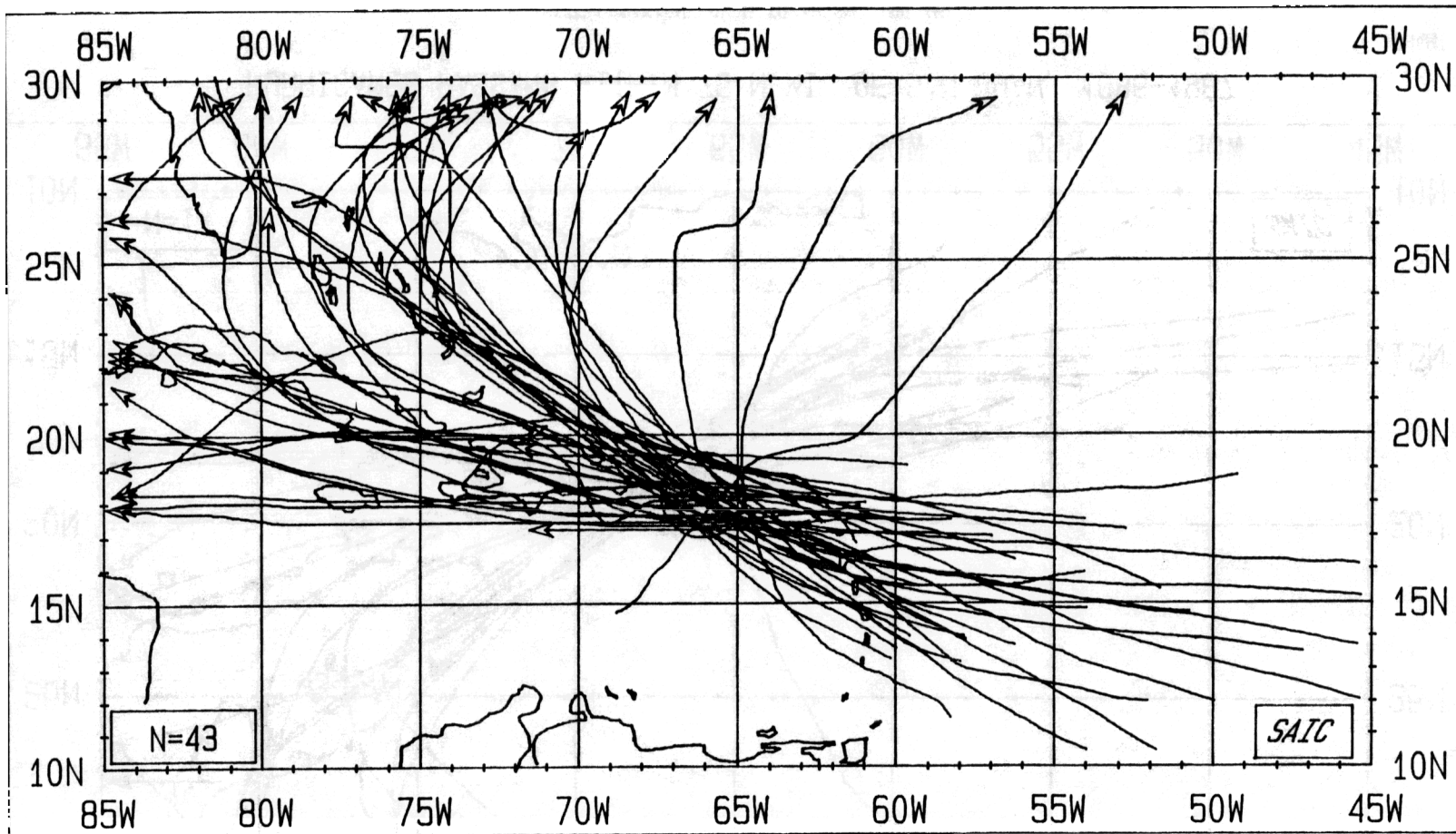
Chart 2 (Fig. 2) shows the tracks of the 43 tropical cyclones identified in Chart 1; that is, those storms which passed through the plotted circular area over the 102-year period, 1886-1987. These include both hurricanes (winds ≥ 64 knots) and the weaker tropical storms ($34 \leq$ winds < 64 knots). The area covered by this chart is assigned by the user. In this connection, it is well to include an area large enough so as to provide sufficient visual up- and down-stream information about the storm tracks.

Beneath the chart appears the comment, "site location moved to 18.2N, 66.1W". This position, rounded off to the nearest tenth of a degree is about 15 n.mi. south-southwest of the actual position of 18.4N, 66.0W, as initially specified by the user. This new position is referred to as an "adjusted" site location. All subsequent program computations are reference the adjusted site.

6.2.2 Technical Discussion (Wind Asymmetries)

The purpose of the adjustment is to account for average storm asymmetries in the wind circulation. In the northern hemisphere, winds are typically higher on the right side of a storm (looking toward the direction of motion) than on the left. This is due to interactions between the rotational effects of the winds and the forward motion of the entire storm envelope. Thus, for the San Juan case, where storms are moving predominantly from the east-southeast towards the west-northwest, a

⁵ On some plot renditions of HURISK, columns 9 and 10 are combined into a single column 9.

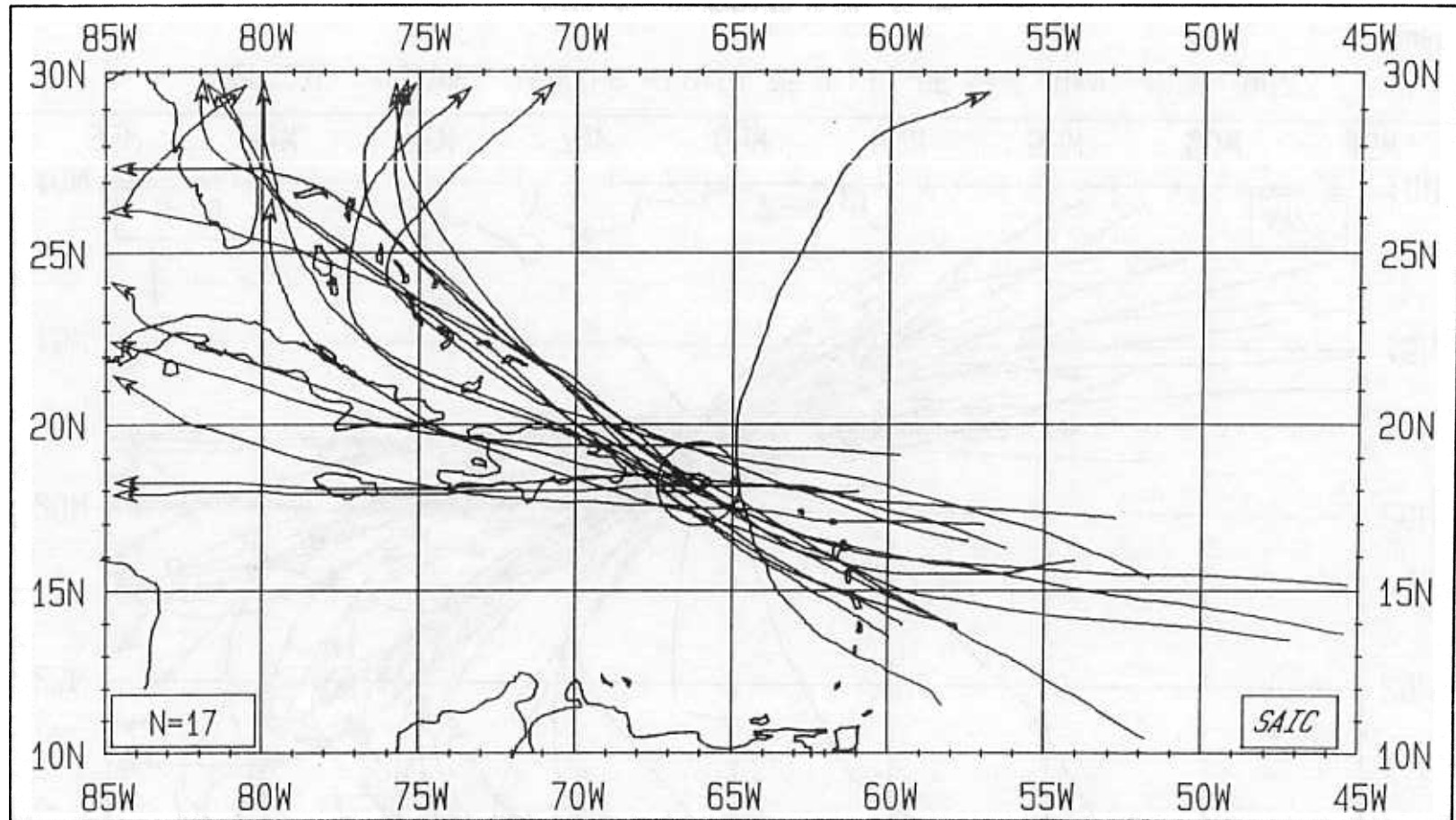


TROPICAL CYCLONES PASSING WITHIN 75 N.MI. OF SAN JUAN, 1886-1987

(SITE LOCATION MOVED TO 18.2N, 66.1W)

CHART 2

Fig. 2. Tropical storm and hurricane tracks



HURRICANES PASSING WITHIN 75 N.MI. OF SAN JUAN, 1886-1987

(SITE LOCATION MOVED TO 18.2N, 66.1W)

CHART 3

Fig. 3. Hurricane tracks

storm passing a given distance to the north-northeast of the site will be expected to produce less wind at the site than a storm which passes at the same distance to the south-southwest. Additional technical discussion on this subject, along with illustrations, is provided by Schwerdt et al. (1979).

To compensate for wind asymmetries, the site is moved in a direction 90 degrees to the left of the average storm vector heading which, for this site, is towards 291 degrees (see chart 6). Thus, the new site is located towards $(291 - 90) = 201$ degrees from the present site. The distance along this heading (D) is computed from,

$$D = W_v/W_s \times \text{RMW} \quad (1)$$

where W_v is the mean vector translational speed of the 43 storms which have effected the site, W_s is the average (scalar) speed of the storms and RMW is the average radius of maximum winds for the storms. From Chart 6, $W_v = 12.4$ knots, $W_s = 13.2$ knots, RMW (from Chart 7) = 16 n.mi. and D computes to approximately 15 n.mi. Thus, the site is moved 15 n.mi. south-southwest (towards 201 degrees) from the initial site location and the 43 storms shown on Chart 2 are reference the adjusted site. A program option for bypassing this procedure is available.

The quantity W_v/W_s , contained in Eq. (1) is sometimes referred to as "wind constancy" or "wind steadiness" and is further discussed by Crutcher and Quayle (1974). Possible values range from zero (when storms move through an area from virtually all directions) to 1.0 (when storms always move from exactly the same direction).

CHART 3

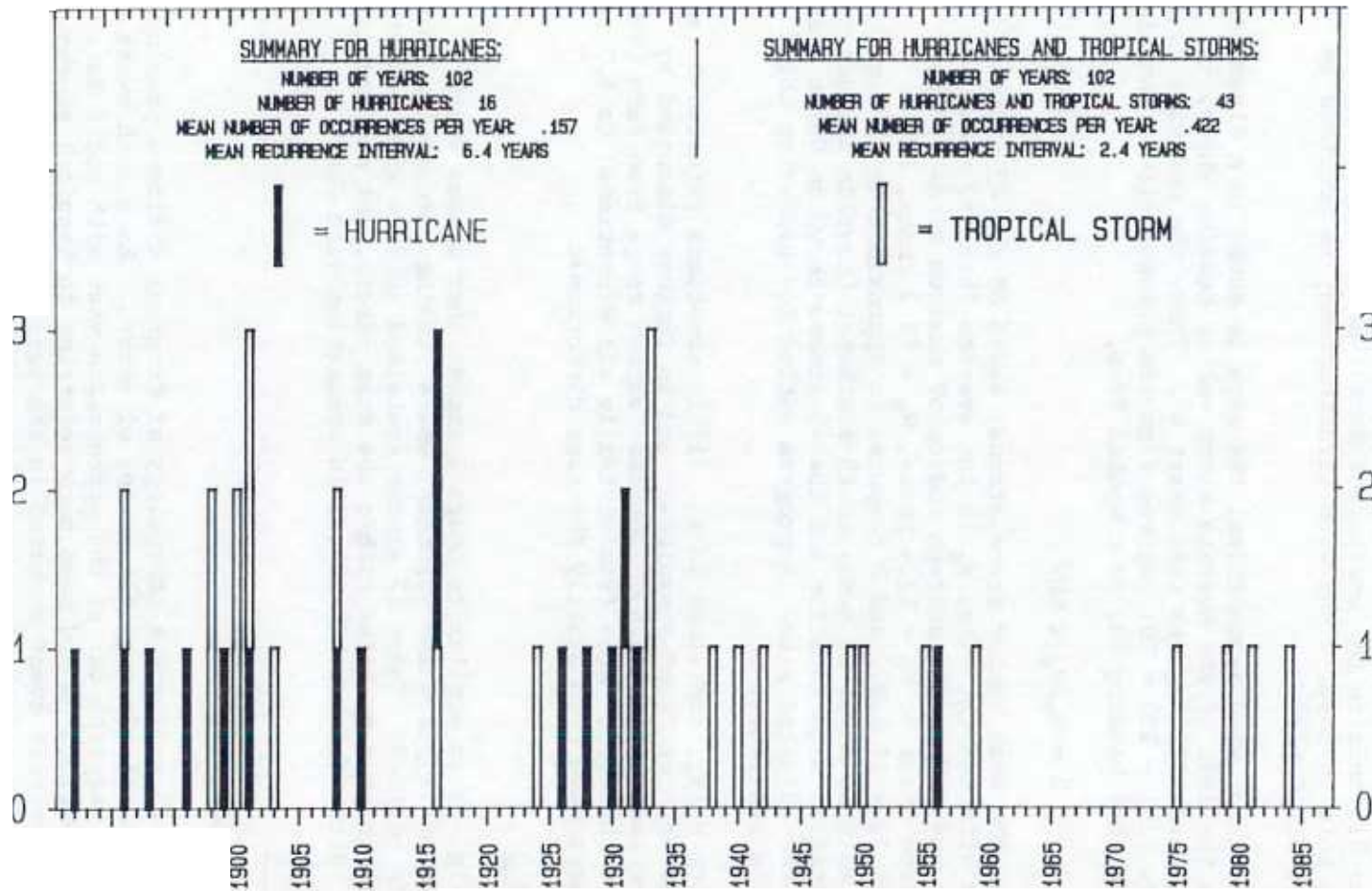
Chart 3 (Fig. 3) is similar to Chart 2 except that storms which failed to exhibit hurricane strength, while passing through the scan circle, are omitted. These 17 storms contained surface winds of at least 64 knots at some point within the scan circle, not necessarily at the site. Site winds are discussed in connection with Chart 9.

CHART 4

6.4.1 Chart Description

Chart 4 (Fig. 4) presents a chronology of tropical cyclones passing within the scan-circle over the period of record. Each such event is depicted as a vertical bar at the appropriate year with solid bars referring to hurricanes and open bars referring to tropical storms. For example, a hurricane event occurred in the year 1887; there were no events in the three following years while one hurricane and one tropical storm event each occurred in the year 1891.

The upper left and right insets, respectively, give additional summary information for hurricanes and for hurricanes and tropical storms combined. The mean number of occurrences per year is simply the total number of storms over the period of record divided by the total number of



TROPICAL CYCLONES PASSING WITHIN 75 N.MI. OF SAN JUAN, 1886-1987

(Note: Storm intensity is determined at time of closest approach to site)

CHART 4

Fig. 4. Chronology of tropical cyclone events.

years. The "mean-recurrence-interval" (MRI) is the reciprocal of this quantity. It can be noted here that the total number of hurricanes is specified as 16, one less than that given in the previous chart. As discussed earlier, this difference results from storm number 29 (see Fig. 1) being at or above hurricane force within the scan-circle but not meeting this condition at CPA.

6.4.2 Technical Discussion

6.4.2.1 A statistical pitfall - This example for San Juan illustrates one of the pitfalls of statistical analysis. If the 102-year period of record is sub-divided into two 51-year periods, 1886-1936 and 1937-1987, it can be noted that 15 of the 16 hurricane events occurred in the first half of the period. Thus, if information through 1936 had been used to estimate the tropical cyclone climate over the second 51-year period, a very large discrepancy would have been noted between forecast and observed conditions.

6.4.2.2 Applicability of Poisson distribution - It can be shown that the observed discrete frequency of tropical cyclone events, as shown in Chart 4, can be described by the Poisson distribution (Xue and Neumann, 1984). This distribution is mathematically defined as,

$$P(x) = e^{-m} m^x / x! \quad (2)$$

where $P(x)$ is the probability ($0 \leq P \leq 1$) of exactly x events over some interval, m is the mean number of event occurrences over the interval, e is the base of natural logarithms and the symbol $(!)$ designates x -factorial. In reference to Chart 4 (Fig. 4), the question might arise as to the probability of two events (where an event is defined as a tropical storm or hurricane within 75 n.mi. of the site) in a single year. The mean of the event has already been defined in Fig. 4 as 0.422 occurrences per year. From Eq. (2), the probability of this event occurring exactly twice in a single year is given by,

$$P(2) = e^{-.422} \times .422^2 / 2! = 0.058;$$

or, 5.8%. It can be noted that the event occurred in 5 of the 102 years (1891, 1898, 1900, 1908 and 1931) giving an observed frequency of 5/102 or 0.049. This is quite close to the value of 0.058, predicted by Eq. (2).

Consider a second example. It can be noted in Fig. 4, that there were 70 of the 102 possible years when the event did not occur giving an observed frequency of 70/102 or 0.686. From Eq. (2), the probability of this event is computed to be 0.656. Again, this computed value is in good agreement with the observed value.

There are sound statistical reasons for using the probabilities predicted by Eq. (2) rather than the relative frequencies with one of the main motivations being that inferences about an event can be made outside the range of observations -- for example, the occurrence of ≥ 4 events in a single year where the event is again defined as a tropical storm or hurricane passing within 75 n.mi. from San Juan. In the context of Eq. (2), this would be given by,

$$P(\geq 4) = 1.00 - P(0) - P(1) - P(2) - P(3) \approx 0.00094 \quad (0 \leq P \leq 1)$$

which is equivalent to a mean recurrence interval of about once every 1062 years $[1/P(\geq 4)]$ for this event. It is important to realize here that these estimates assume that the San Juan tropical cyclone climate over the past 102 years will remain unchanged over the next n-years. It also assumes that individual occurrences of events are independent. While the latter assumption is reasonable, the former is not (see previous section, 6.4.2.1). Further discussion on this topic is beyond the scope of the manual and the reader is referred to standard statistical texts such as Hahn and Shapiro (1967). Further application of the Poisson distribution function to tropical cyclone climatology is discussed in connection with Charts 10 and 11.

CHART 5

Chart 5 (Fig. 5) gives information relative to seasonal variation in storm occurrence. Along the horizontal axis, the chart is subdivided into 52 seven-day periods but with the last period, Dec. 24 - Dec 31, containing 8 days. The dates on the Chart refer to the time that the storm was closest to the site. The median occurrence date (50% of the cases fall below this value and 50%, above) is also specified. These dates correspond to dates given in Chart 1.

CHART 6

The distribution of directions towards which the ensemble of storms were moving at the time of their closest approach to the site is given in Chart 6 (Fig. 6). The horizontal axis is subdivided into 10-degree class intervals while the frequency of occurrence, given in percent of cases, is given along the vertical axis. Solid bars are for hurricanes and open bars are for tropical storms. Directions from which the storms were moving (according to a 16-point compass) are also indicated. Additional summary information relative to translational directions and speeds, is included along the top of the chart. The resultant (vector) speeds are always less than or equal to the mean (scalar) speeds. These two quantities are equal only when all storms move from exactly the same direction. The vertical arrow below the ESE (east-southeast) marker refers to the resultant storm direction (towards 291 degrees).

The ratio of the resultant speed divided by the mean speed is sometimes referred to as a "wind-constancy" or "wind-steadiness" value (see Section 6.2.2). In this example, the wind-constancy for the all storm category is $12.4/13.2 = 0.94$. This is a rather high value, indicating that storms in this area do not deviate very much from west-northwesterly headings. In general, relatively high values of constancy are found at low latitudes, where the storms are most likely to be embedded in a basic easterly (from the east) "steering" current and also at high latitudes where storms are typically embedded in a basic westerly (from the west) current. At intermediate latitudes (25 to 35 North), average constancy values are almost always below 90% and, in some areas, they aver-

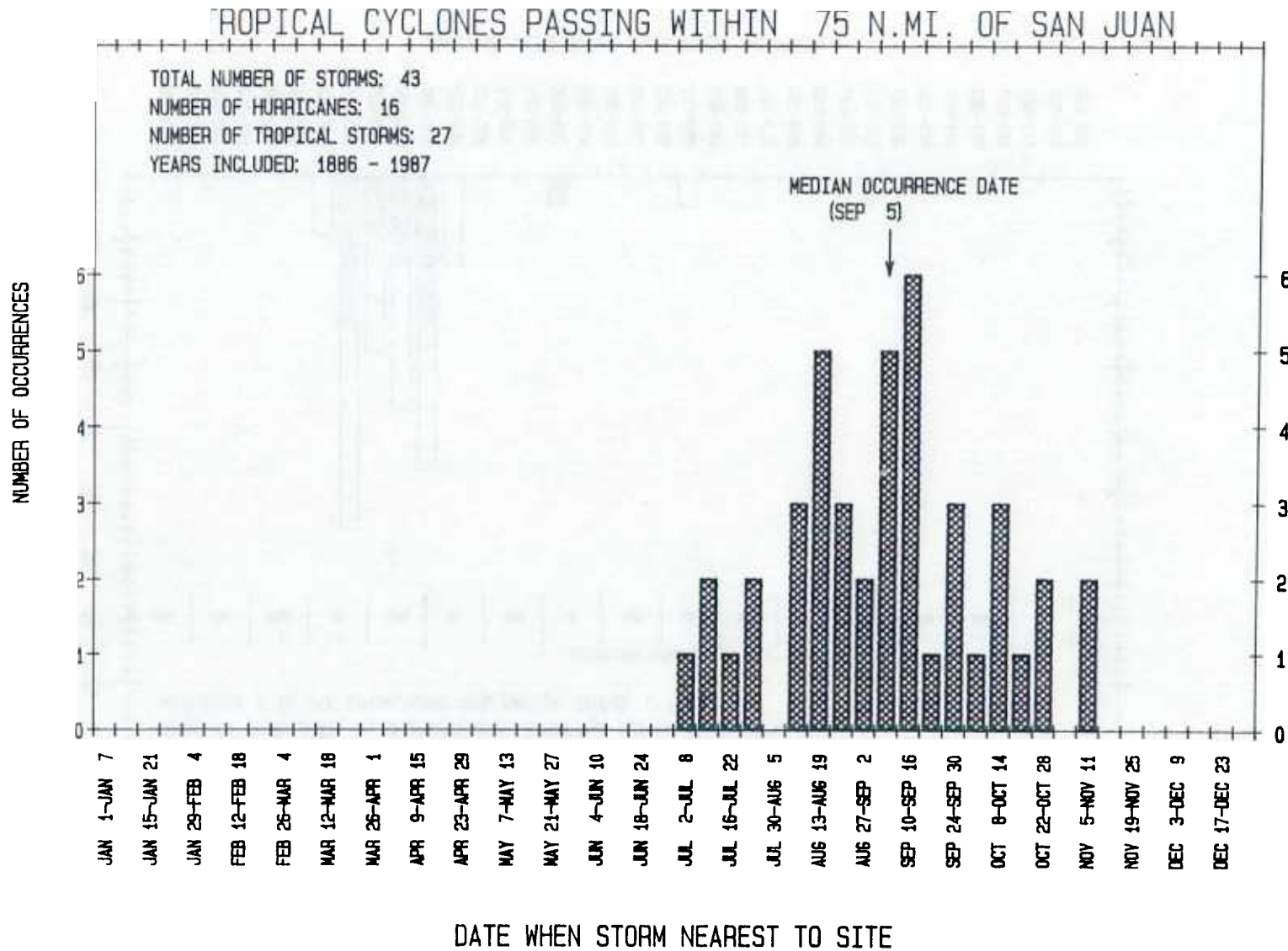


CHART 5

Fig. 5. Intra-seasonal variation in storm occurrence

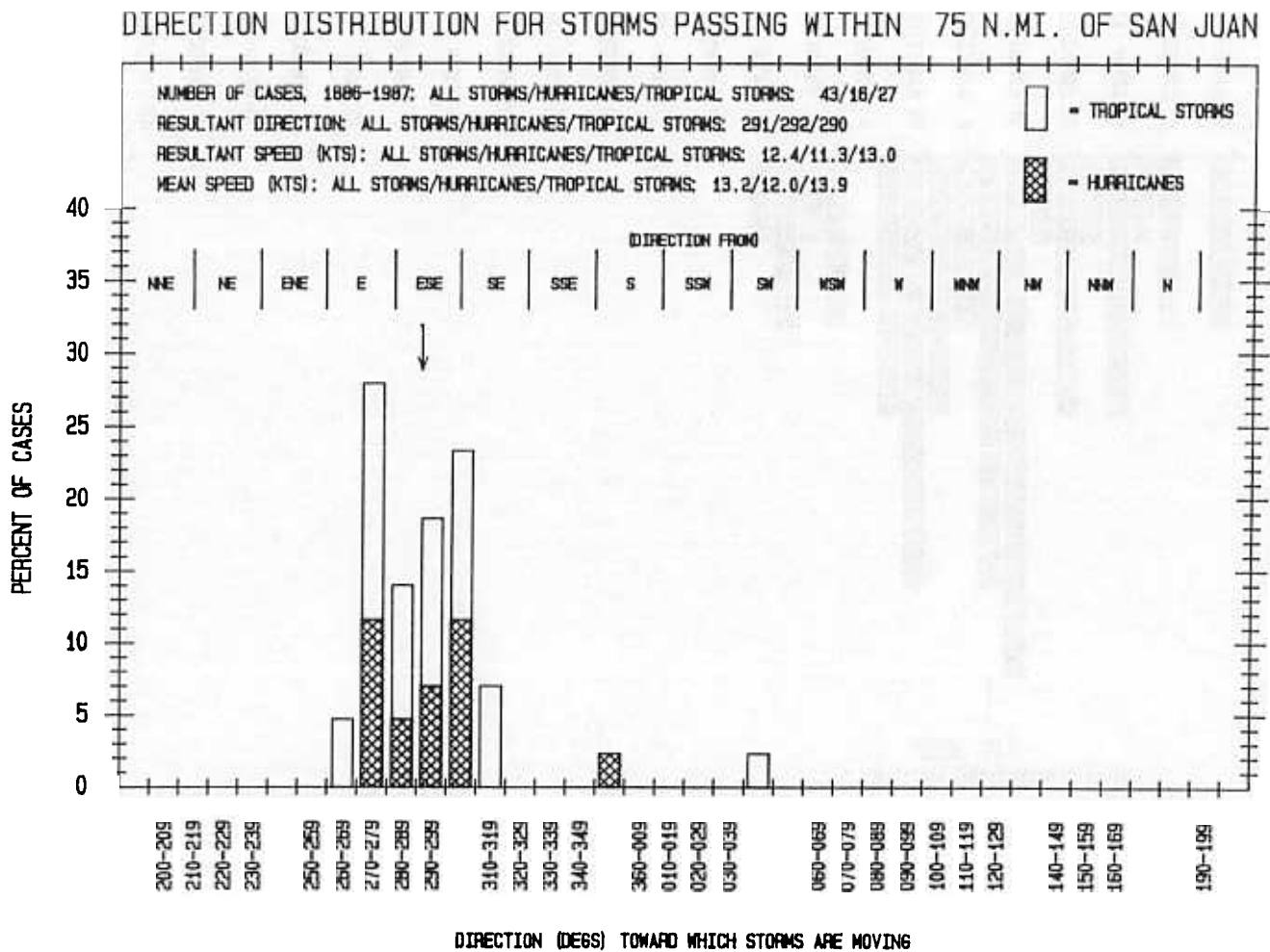


CHART 6

Fig. 6. Distribution of storm headings

rage below 75% (Hope and Neumann, 1971). In these latitudes, environmental storm steering forces are apt to fluctuate between easterly and westerly.

6.7 CHART 7

Up to this point, charts have referred to storms passing within a 75 n.mi. radius of a site. The next 2 charts, that is, Charts 7 and 8, are prerequisites for the computation of return periods of winds at the site itself which is addressed by Chart 9. Computation of tropical cyclone return periods is quite complex and no attempt will be made in section 6 to describe the procedure. Although some technical material will need to be introduced, the focus, at this point, will be on proper use of the charts, rather than technical understanding. For those interested in following through with the procedure, a theoretical discussion of the return period procedures is given as an Appendix.

6.7.1 Chart Description

Chart 7 (Fig. 7) provides one of the important links between winds near the center of a tropical cyclone and winds at the site itself. Up to this point, reference has been made to the number of storms passing within a scan-circle of 75 n.mi. radius. Obviously, scan-circles of lesser radii would encompass fewer storms. The radius of the scan-circle is represented by the horizontal (x) axis while the number of storms passing within this distance is represented by the vertical (y) axis. It has already been pointed out that 43 storms have passed within a scan-circle radius of 75 n.mi. from the site and this amount is represented by the upper-right most data-point on the chart. In column 8 of Chart 1, the closest point-of-approach of each storm to the site was given. These points, summed cumulatively, are also plotted on Chart 7. Thus, for example, there are 24 storms which have passed within 40 n.mi., 19 within 30 n.mi., etc.

6.7.2 Technical Discussion

6.7.2.1 Line of best fit - The shape of this cumulative distribution is a function of the storm climatology for the area. At some sites, the increase of storm count with increased area is approximately linear (as it is here) while at others, it is non-linear, but always monotonic. Attempts at fitting several mathematical functions to these data led to a selection of a simple second-order polynomial function as a satisfactory line of best fit. The function, and not the data, is subsequently used in representing the relationship between scan-circle radii and number of storms for the given site. Here, for example, the actual count of storms passing within 75 n.mi. was 43 but the function indicates a better value is 44 storms. The multiple correlation coefficient of the fit is given in the lower right hand corner of the chart and is seen to be 0.993 in this case. Over one hundred of these charts have been examined and the correlation coefficient always exceeded 0.975.

6.7.2.2 A mathematical problem - Occasionally, the polynomial fit is poor near the origin and the function, on rare occasions, indicates a negative number of storms passing within a finite distance from the

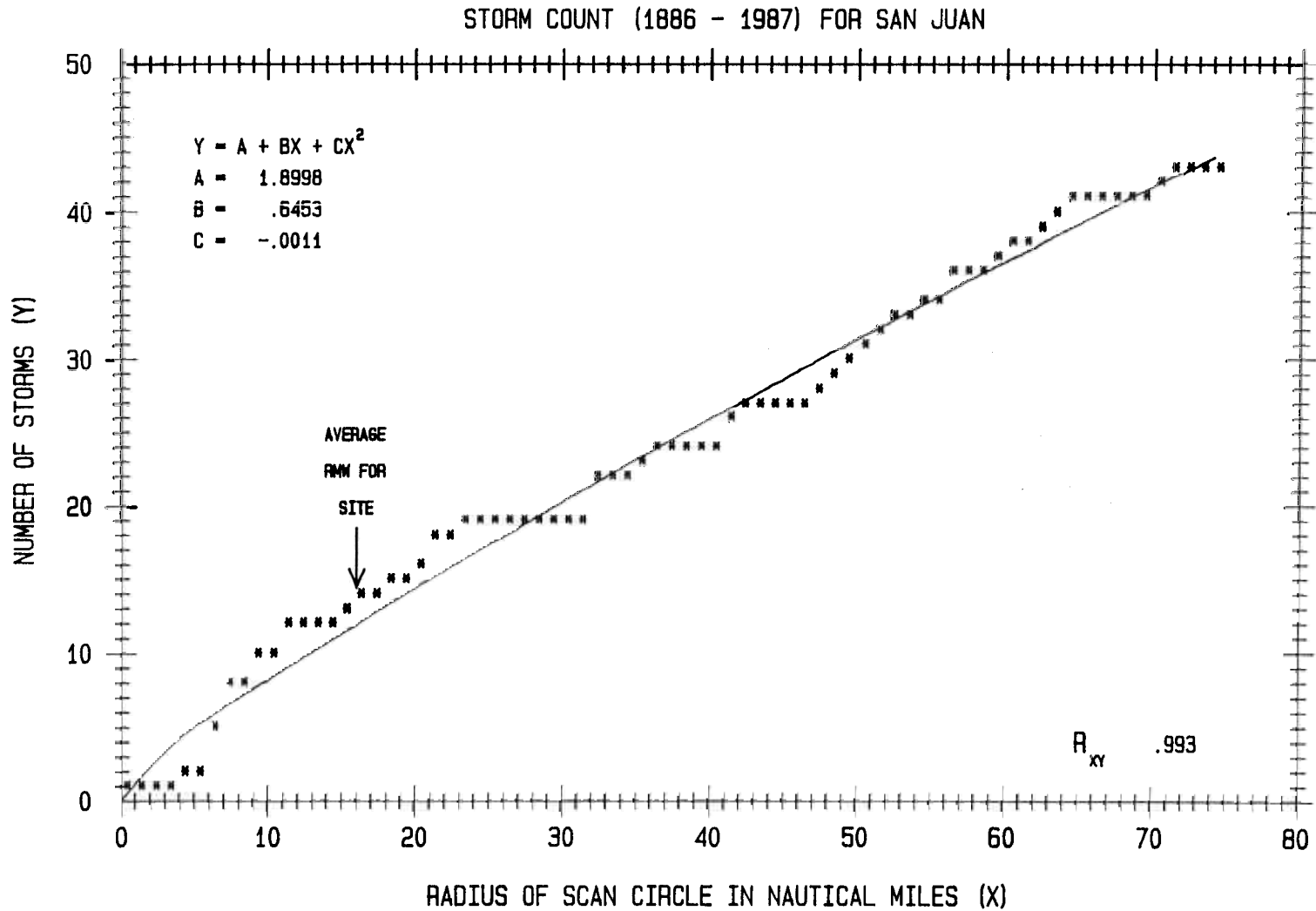


CHART 7

Fig. 7. Storm count as a function of scan-circle radius

site. This impossible condition could lead to subsequent computational problems and the decision was made to constrain the function to locally pass through the origin. Since this always occurs at a scan-circle radius of less than the average radius of maximum wind for the site, it is of no consequence in later mathematical return-period computations.

6.7.2.3 The role of RMW - The radius of maximum wind for the site (see Appendix 1 for method of obtaining this quantity) is shown at its proper location on Chart 7. The significance of the RMW is that the maximum wind of storms which pass at lesser distances from a site would likely be observed at the site itself. Thus, in the example shown here, approximately 12 of the 43 storms which have affected this site should have passed near enough for the site to have observed the maximum wind assigned to the storm. For storms which pass at greater distances, standardized but appropriate horizontal wind profiles would be needed to assess winds at the site. In actual practice, the situation is much more complex in that the storm intensity, the radius of maximum wind, the distance of the storm center from the site, frictional influences, as well as other parameters, are continuously varying and one must resort to computer simulation (Monte-Carlo procedures) for a reasonable solution. This is further discussed in the Appendix.

CHART 8

Four parameters which potentially determine the wind observed at a site from a given storm have been discussed or mentioned in the preceding section: (1) the distance a storm passes from a site, (2) the radius of maximum wind, (3) the horizontal wind profile and (4) frictional wind effects. Another obviously important parameter is the storm intensity. This is specifically addressed in Chart 8 (Fig. 8).

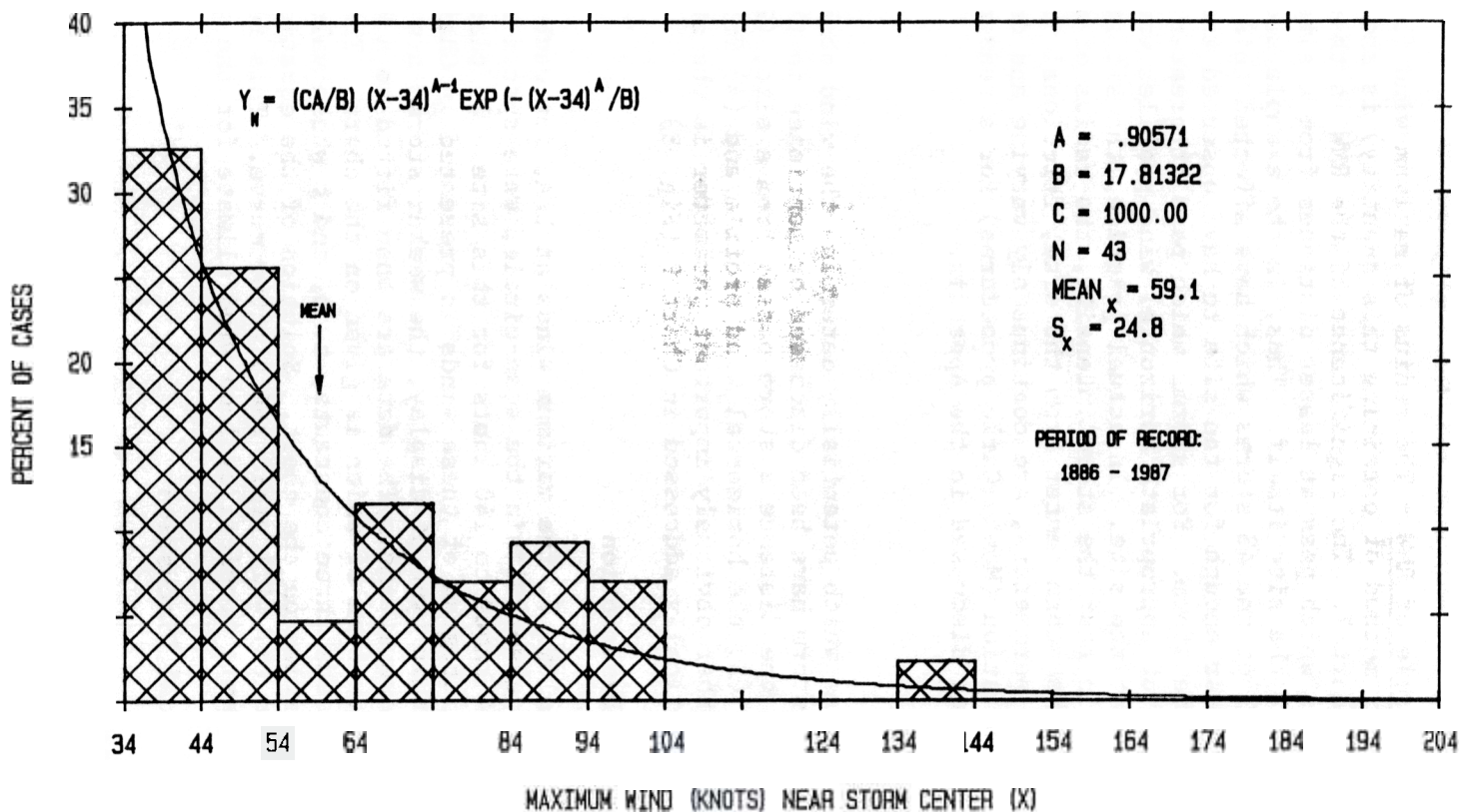
Chart Description

In Chart 1, column 7, the maximum winds at CPA, for each of the 43 storms which passed within the scan-circle, were specified. These ranged from 34 knots to 140 knots for this site. In class intervals of 10 knots, a histogram of these winds is presented in Chart 8. As is typical with this type of display, the weaker storms are far more common than the intense storms. The data are then fitted to a Weibull distribution, the equation of which is given on the chart. The mathematical function contains three constants, a, b, and c whose values (estimates) are also specified on the chart. Solution of the equation with various values of wind (x) will yield the plotted curve. This function describes the basic tropical cyclone wind climate for the given site.

Technical Discussion

6.8.2.1 Choice of Weibull distribution - The Weibull distribution, often used in time-to-failure analysis, has recently been used by several authors (see Appendix) to describe tropical cyclone maximum wind distribution. However, it is believed that the simpler Gamma distribution, (see discussion under Chart 12) could also have been used. Indeed, earlier versions of HURISK did use the Gamma distribution. The shape (a) and scale (b) parameters of the distribution were determined using maxi-

WEIBULL DISTRIBUTION FITTED TO HISTOGRAM OF OBSERVED MAXIMUM WINDS
 FOR TROPICAL CYCLONES PASSING WITHIN 75 MI OF SAN JUAN



CHART

D: bu imum winds th

imum likelihood methods as described by Abernethy et al. (1983). In practice, both the Weibull distribution and the Gamma distribution approach the simpler exponential distribution depending on the value of the shape parameter. This is a rather typical situation over portions of the tropical cyclone basin where weak storms far outnumber stronger storms.

6.8.2.2 Adequacy of fit - The Weibull distribution fit to the data, at least in the visual sense, is reasonably good. The apparent observational deficit in the class interval 54 to 64 kts could well be explained by data deficiencies, biases or chance departures. Further discussion on this subject is beyond the scope of the manual although some further treatment is given in the Appendix.

6.9 CHART 9

6.9.1 Chart Description

6.9.1.1 Wind return periods for site - Chart 9 (Fig. 9) is probably the most useful of the various charts produced by HURISK. Although derivation of the chart is quite complex, usage is relatively simple. The x- (horizontal) axis gives the maximum wind at the site while the y- (vertical) axis gives the return period of this wind in years. It is necessary here to again point out that the winds referred to in Chart 9 and throughout the text represent a 60-second average. Shorter period gusts/lulls in the wind are apt to be much higher/lower than this averaging period. A 1-second gust, for example, is typically 1.25 times higher than a 60-second average. A graphical procedure for converting from one averaging-time to another can be found in Simiu and Scanlan (1978) and in ANSI (1982). Also discussed in the former reference is the term, "fastest-mile", often used by wind engineers as a return period measurement unit.

The chart is designed to give return period estimates of given winds both at the site itself and over an area around the site. Site winds are given by the sloping dashed line, the position of this line having been determined largely by the computer simulation methodology described in the appendix. For example, the return period of at least 64 knot (hurricane force winds) is read as 24 years and of at least 100 knot winds, 153 years. By entering from the vertical axis, n-year events can be determined. For example, the 50-year tropical cyclone event is read as 79 knots (91 mph) while a 100-year event is read as about 92 knots (106 mph). Further discussion of n-year events is given below in section 6.9.1.3.

6.9.1.2 Areal wind return periods - Chart 9 is also designed to provide tropical cyclone wind return periods within areas centered on the site and extending outward through a radius of 75 n.mi. For example, a 100-knot storm can be expected to pass within 75 n.mi. of the site about once every 30 years and within 10 n.mi. of the site every 160 years. It should be noted here, however, that storms passing just outside the bounds of the scan-circle area could also bring 100 knot winds within the bounds of the area. This procedure, therefore, can only be used with some qualification (see section 6.9.1.4).

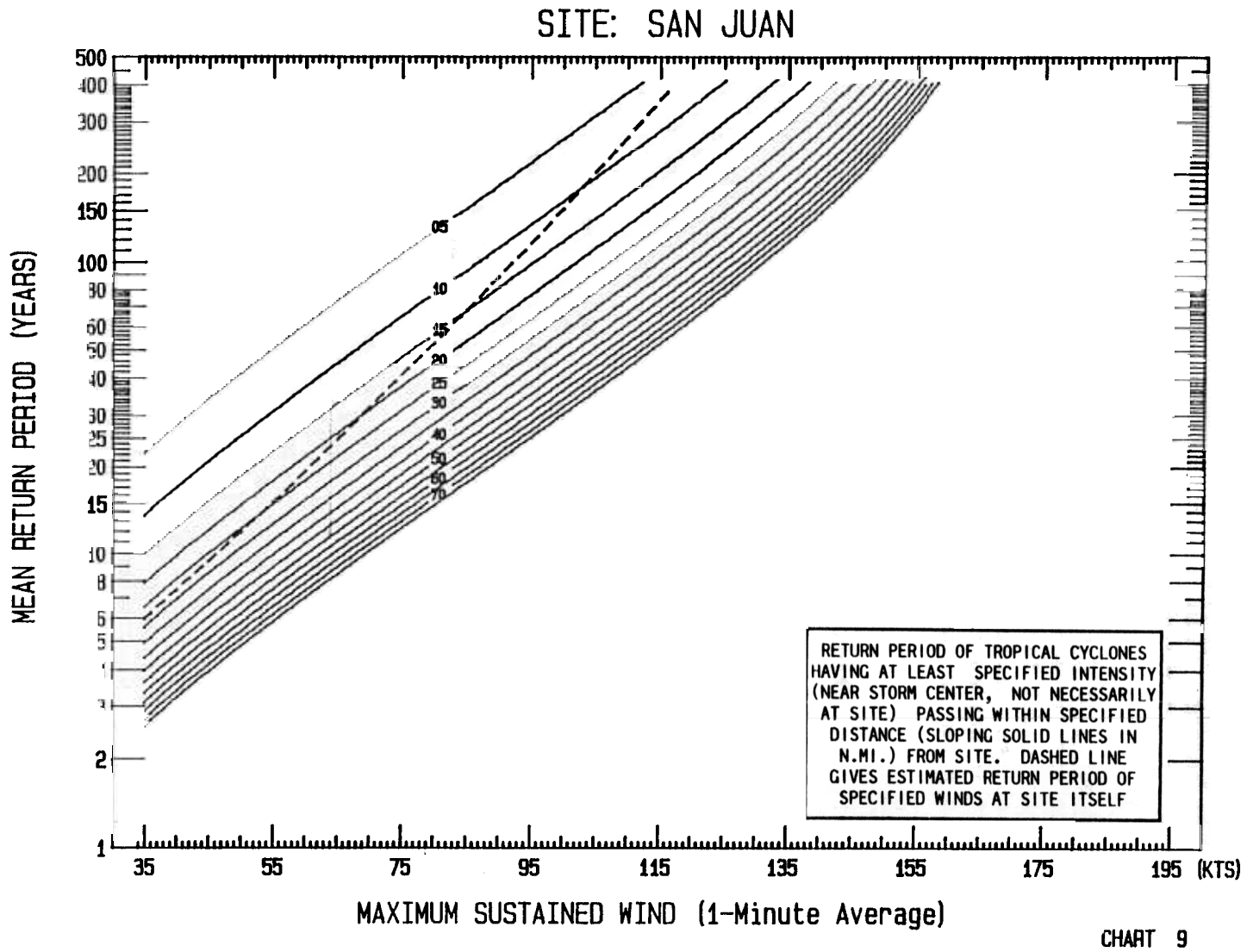


Fig. 9. Areal and site return periods of specified winds

6.9.1.3 N-year events - The subject of return periods is closely tied to n-year events. These are defined as events (strong winds, excessive rainfall, etc.), the magnitude of which are equaled or exceeded, on the average once every n-years. The term "on the average" is important here. An n-year event need not occur once every n-years. For example, in Chart 4, it was pointed out that the mean recurrence interval (return period) of tropical cyclones having at least 34 knots of wind passing within 75 n.mi. of San Juan was 2.4 years; that is 43 occurrences of the "event" over 102 years. However, it can be noted that there were three years (1901, 1916 and 1933) when the event occurred three times each year and long spans of years when the event did not occur at all, for example, the 15-year span from 1960 through 1974.

Similarly, a 100-year event need not occur every 100 years. It can be shown from the binomial distribution (and, approximately, from the Poisson distribution) that the chance of a 100-year event occurring or being exceeded in 100 years is about 63%; in 200 years, 87% and in 500 years, 99.3%, etc. The chance of the event not occurring during the specified span would be 100% minus those values or, 37%, 13% and 0.7%, respectively.

An n-year event is often referred to as an event having a 1/n chance of occurring in a single year. Thus, a 50-year event has a 2% while a 100-year event has a 1% chance of occurring in a single year.

6.9.1.4 Further applications of Chart 9 - It has already been demonstrated that the return period of 64 knot sustained (hurricane force) winds at San Juan is 24 years. This is a point probability; that is, it is applicable only to a given location in the vicinity of San Juan. However, there is often the need to assess probabilities over larger areas. Obviously, the larger the area, the larger will be the probability of observing a given wind somewhere within the area. As an example, consider the question, "What is the return period of, say, hurricane force winds somewhere over the entire island of Puerto Rico"? Although the HURISK program was not specifically designed with this application in mind, sufficient data are available to provide a reasonably reliable estimate.

To activate this procedure, the radius of a circle which yields the same area as the land mass of Puerto Rico is needed. Areas of land masses are typically given in square statute miles while the radius needed here must be in nautical miles; Eq. (3) can be used to effect this conversion;

$$Re = 0.49 \sqrt{\text{Area}}, \quad (3)$$

where Area is in units of statute miles and Re is returned in units of nautical miles. The area of Puerto Rico is approximately 3435 square statute miles and from Eq. (3), an equivalent radius (Re) would be 28.7 nautical miles. To estimate the return period of hurricane force winds at any point over the island of Puerto Rico:

- (1) Draw a vertical line on Chart 9 through 64 knots (or through any intensity of interest).
- (2) Note the intersection of this with the dashed point probability line and further note the value of the scan-circle radius at this point. In this example, this is found to be about 22 n.mi.
- (3) To this value, add the 28.7 n.mi. equivalent radius to obtain an adjusted radius of $22 + 28.7 = 50.7$ n.mi.
- (4) Re-enter Chart 9 and read the return period (along the 64 knot vertical line) associated with the 50.7 n.mi. and read about 11 years. This is the estimate of the return period of hurricane force winds anywhere over Puerto Rico.

Thus, the return period of at least hurricane force winds at San Juan is computed to be 24 years, while, over the island as a whole, it is computed to be near 11 years. Reliable records maintained in Puerto Rico indicate that between 1871 and 1987, 12 hurricanes (years 1876, 1891, 1893, 1896, 1899, 1901, 1916, 1926, 1928, 1931, 1932, 1956) have passed over the island. This is a mean recurrence interval of about 10 years, suggesting that the estimate from Chart 9 is reasonably reliable.

As a further example of this procedure but using a 100-knot wind threshold, the vertical line through 100 knots intersects the point-probability line at about 11 n.mi. Adding 28.7 to this value gives an adjusted radius of 39.7. The return period equivalent to this distance is about 52 years. Thus, 100 knot sustained winds should be expected somewhere over Puerto Rico about once every 52 years. This compares to a return period of 153 years for the occurrence of 100-knot sustained winds at San Juan, itself.

This procedure of obtaining areal probabilities should be applicable to any area providing the shape of the land-mass is approximately circular. The procedure would probably be invalid, for example, for the island of Eleuthera where the island's length far exceeds the width. The validity of the procedure is also dependent on the prevailing storm heading in the area relative to the shape of the land mass. Finally, It would not be valid for very large landmasses where the area exceeds that equivalent to a radius exceeding about 60 n.mi. Universal applicability of this procedure has not been extensively tested and the objective procedure would need to be tempered with some subjective judgement.

6.9.2 Technical Discussion

6.9.2.1 Areal return periods (mathematical derivation) - The actual positioning of the family of solid lines on Fig. 9 is a function of the Weibull distribution of winds (Chart 8) and the storm-count distance function (Chart 9). The procedure assumes that these two functions are independent. Since neither the direction of storm approach nor the direction of storm induced winds are considered in HURISK, this is a reasonable assumption. In effect, this assumption states that a storm which passes, say 20 n.mi. from a site, could just as well have passed over the site.

As used here, the mathematical formulation of the Weibull distribution (Tsokos, 1972) is given by,

$$f(x) = c(a/b)(x-34)^{a-1} e^{[-(x-34)^a/b]}$$

where x is the maximum sustained wind and a and b are constants. These constants, often referred to as shape and scale parameters, respectively, are determined from the actual wind data using maximum likelihood estimates (Abernethy et al. 1983). An additional constant, c , as specified on Chart 9 is used as a scaling factor if the area under the bars and under the curve is other than 1.0, as it is here (area = 10kts x 100% = 1000). Eq. (4) can be integrated to obtain the probability of any range of winds.

As a specific example, consider the probability of the wind exceeding 100 knots using the values of a and b shown in Fig. 8 (Chart 8) and where $f(x)$ is given by Eq. (4),

$$p(>100) = 1 - \int_0^{100} f(x) dx = 0.0764.$$

Thus, 7.64% of the storms passing at some distance from the site would be expected to have maximum sustained winds of at least 100 knots. The actual number of storms passing within various distances from the site is given by the polynomial function described on Chart 7. Using this function, the number of storms passing within 75 n.mi. from the site (over the 102 year period of record) is 44.0. This is slightly greater than the observed count of 43 storms. Thus (from equation 5), 7.64% of these 44 storms or 3.36 storms should have maximum winds exceeding 100 knots. Since this occurred over a 102 year period, the mean recurrence interval or return period is given by $102/3.36$ or once every 30 years. It can be noted that this is the value read from Fig. 9.

Similarly, the number of storms passing within 30 n.mi., is given as 20 on Fig. 7. Using the same methodology as above, this is equivalent to a mean recurrence interval or return period of 66 years (for the 100 knot threshold) and this value can similarly be obtained from Fig. 9. All additional values given on Chart 9 (Fig. 9) were obtained in this manner.

6.9.2.2 Maximum possible storm intensity - The Weibull function, illustrated in Chart 8 is unbounded at the upper end; thus, the distribution would give a finite probability for winds of, say, exceeding 200 knots. Because of natural controls, it is not likely that a tropical cyclone could reach that intensity. It would not be proper to truncate the distribution at some wind value since this would effectively give an area under the function less than its true value. The method used here was to initially integrate the function through 175 knots and then to use this adjusted area rather than the true area as the basis for the computations.

There were theoretical and practical reasons for using the 175 knot threshold wind value. While most meteorologists agree that there is some upper bound to maximum possible hurricane intensity, there is no universal agreement as to what this limit might be and estimates might

range between 150 and 200 knots (1-minute average). The lowest pressure ever recorded in a tropical cyclone was 870 millibars but this was over the Western North Pacific where tropical cyclones are more severe, on the average, than over the Atlantic. The maximum wind recorded on the HURDAT⁵ data set is 165 knots and the lowest pressure, 892 millibars. Emanuel (1986) presents a theoretical estimate of somewhat less than 880 millibars central pressure (equivalent to about 175 knots) for the Atlantic. Accordingly, this latter value was used in HURISK. Thus, without some modification, HURISK cannot be used to estimate return periods of extreme duration (for example, a 10,000 year return period), since this somewhat arbitrary cutoff value of 175 knots would flavor the results.

6.9.2.3 A simplified procedure - In a previous section (6.9.2), the derivation and positioning of the family of areal return period lines on Chart 9 was discussed. The orientation, spacing and gradient of these lines is highly variable and depends on the storm climatology for a given site.

The positioning of the the dashed line, giving the return periods at the site itself, is much more complex and, since it was accomplished through an empirical computer simulation procedure, a strict mathematical formulation is not possible. After running the simulations for a number of sites around the basin, it was noted that the position of the dashed return period line remained reasonably constant relative to the other (solid) lines. After correcting for different average radii of maximum wind from one site to another, the differences became even less.

The above circumstance led to the adoption a simplified procedure whereby the actual position of the dashed line was determined by a multiple regression equation effectively relating the site return period (dependent variable) to radius of maximum wind, intensity, and a variable sensitive to the position of the family of areal return period lines as determined from the simulation. One of the advantages of using the regression equation approach is that the amount of computer time required to run HURISK is reduced by a factor of four. The computer simulation procedure described in the Appendix requires an enormous amount of computation. While this is not a problem on mainframe computer systems, it is, indeed, a problem on smaller systems. As stated earlier, one of the goals of HURISK was to run the program on other than mainframe systems.

On the negative side of the trade-off, the regression equation approach somewhat reduces the accuracy (where the term accuracy is used in the relative sense) of the site return periods. However, any loss in accuracy here is probably commensurate with uncertainties contributed by other assumptions used in the computations and, in particular, with the limited accuracy of the data itself. Extensive testing of the procedure throughout the tropical cyclone basin indicates that the site return periods produced by the program are in reasonable agreement with past

⁵ The term 'HURDAT' refers to the computer data file containing historical tropical cyclone data (Jarvinen et al. 1984).

events. However, since only 102 years of records are available, it is obviously impossible to assess the veracity of the results for periods beyond this interval.

Research on this topic is continuing at the National Hurricane Center and is likely that the position of the dashed point-probability line could be modified as additional data becomes available for analyses.

6.9.2.4 Summary of Chart 9 restrictions - As discussed in the preceding section, the site return periods are considered reasonably valid for periods of up to about 100 years. However, Chart 9 contains return period data for periods through 450 years. Users are advised to use these extended data with some reservation. If still longer return periods are needed, it is recommended that the extended return period procedure described in the Appendix be activated for each individual site. Also, it should be possible to further refine the estimates by tuning some of the program input variables (radius of maximum winds, Weibull truncation factor, parameter estimates, frictional influences, etc.) to the given site. It can be shown that small changes in these factors will make rather large changes in the long-term return periods.

6.10 CHART 10

6.10.1 Chart Description

Chart 10 (Fig. 10) is a further application of the Poisson distribution, initially introduced under Chart 4. However, Chart 10 provides specific estimates of multiple occurrences of an event (up to 5) over multiple years (up to 20). In this chart, the "event" is defined as the occurrence of a tropical cyclone having at least 34 knots of wind passing within 75 n.mi. of the site. The number of consecutive years is given along the horizontal (x) axis while the percentage probability of the event occurring is given by the left vertical (y) axis and the percentage probability of the event not occurring is given by the right vertical axis.

On Chart 4, it can be noted that there were 32 out of the 102 years when the event being considered here occurred at least once in a given year. This is a relative frequency of 32/102 or about 31.4% of the years. From Chart 10, the mathematical probability of this event (the total length of the bars over 1-consecutive year column) is read from the left-hand vertical scale as about 34%.

Returning again to Chart 4, it can be further noted that in 24 of the 102 years, the event occurred exactly once per year giving a relative frequency of 24/102 or about 23.5% of the years. From Chart 10, the probability of this event (the length of the narrow bar only) is given as about 27 or 28% of the years.

There are numerous combinations of event occurrence or non-occurrence over various time-frames which are addressable from Chart 10. For example, consider an alternative event -- going for two consecutive years without an occurrence of a tropical cyclone within 75 n.mi. from the site. From Chart 10 (now using the right vertical axis and the 2-year

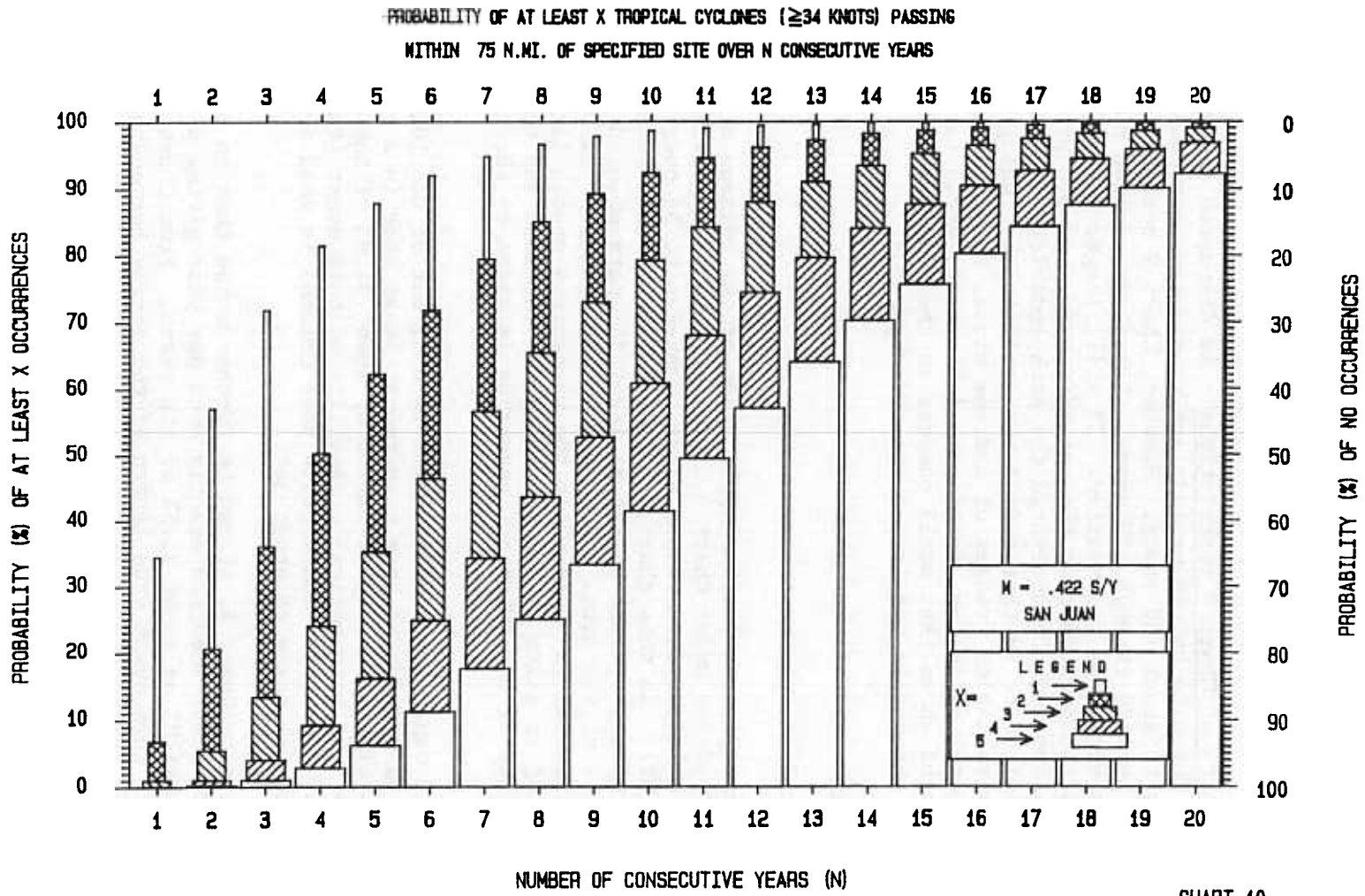


Fig. 10. Poisson probability of multiple tropical storm and hurricane events

column), the probability of this re-defined event is given as about 43%. From Chart 4, with some difficulty, this event can be determined to have occurred on 43 out of 101 available 2-year consecutive periods, 1886-1987. Thus, the estimate of this event from Chart 10 is very close and, indeed, is the preferred estimate.

Consider one final example. What is the probability of going for five consecutive years without a tropical cyclone passing within 75 n.mi. of the site? From Chart 4, this specific event occurred on 14 of the 97 available 5-year spans, 1886 through 1987 giving a relative frequency of 14.4%. From Chart 10, the probability of the newly-defined event (using the 5-year column and the right-hand scale) is determined to be about 12% of the years.

6.10.2 Technical Discussion (Estimated Mean)

As pointed out above, the Poisson distribution (see equation 2 under Chart 4) is used as the basis of the probabilities given in Chart 10. When using the distribution in this manner, the mean of an event must be estimated over the duration of the event. From the last example cited in section 6.10.1, a five-year event is under consideration. It is known from Chart 4 that the 1-year mean of the event is 43 occurrences over the 102 years or 0.422. Thus, the 5-year estimated mean of the event becomes $(43/102) \times 5$ or 2.11 occurrences per 5 years and from Eq. (2), the probability of no occurrences in 5 consecutive years (noting that $0! = 1$) is,

$$P(0) = e^{-2.11} \times 2.11^0/0! = 0.121 \text{ or } 12.1\%$$

6.11 CHART 11

Chart 11 (Fig. 11) is similar to Chart 10 except the event is defined as the number of hurricanes passing within 75 n.mi. from the site which, for this site, totals 17 (see section 6.1.3). For example, the probability of observing this event at least once over a 10-year consecutive period, is read as about 81%.

6.12 CHART 12

6.12.1 Chart Description

Chart 12 (Fig. 12) addresses the speed distribution of tropical cyclones as they pass closest to the site. Each individual storm speed was specified in column 10 of Chart 1. The mean of these 43 individual speeds is given on chart 12 as 13.2 knots and the standard deviation as 5.56 knots. The Gamma distribution, being bounded by zero on the lower and, theoretically, having no upper bounds, was selected as adequately describing the observed distribution. The most frequently occurring speed (mode) is about 10.9 knots. In the subjective sense, these charts are useful when used in comparison with similar representations for other sites or for different category storm classifications for the same site (see discussion under Chart 13).

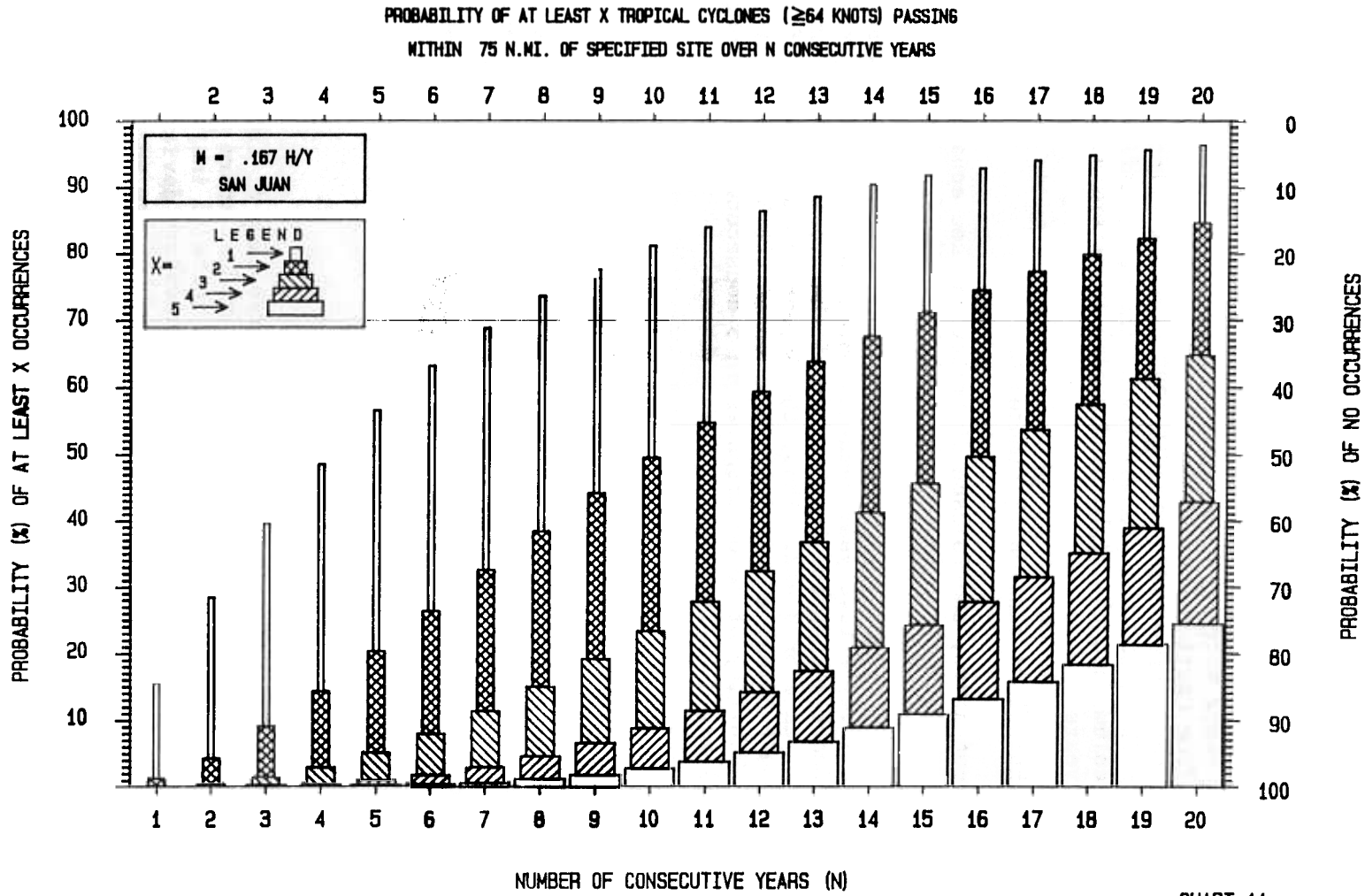


CHART 11

Fig. 11. Same as Fig. 10 except for hurricanes only

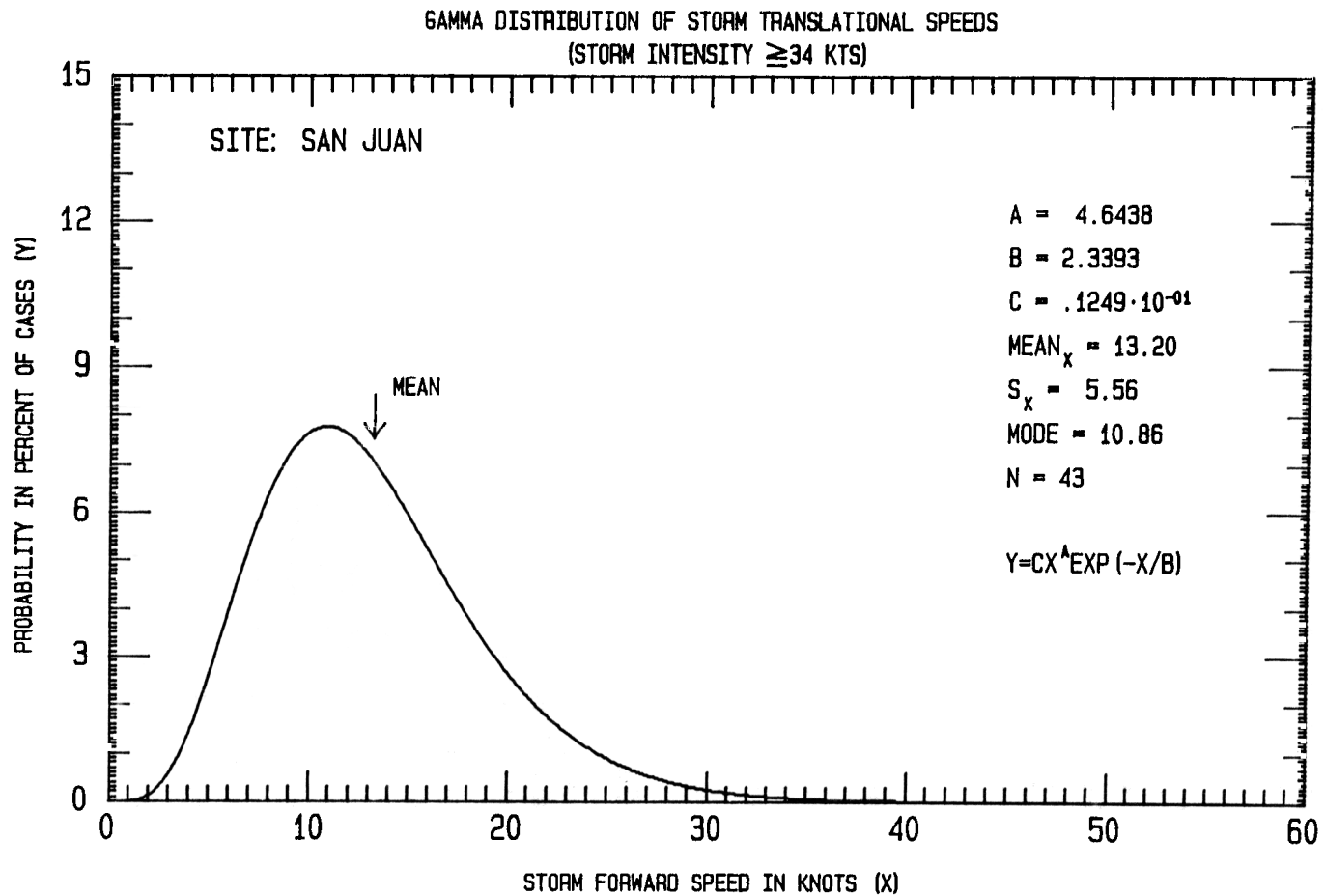


CHART 12

Fig. 12. Distribution of tropical storm and hurricane forward (translational) speeds

6.12.2 Technical Discussion

6.12.2.1 Integration of Gamma distribution - The form of the Gamma distribution used in this study (shown on Charts 12 and 13) is described by Burington and May (1958). The variable 'y' represents frequency of occurrence while 'x' represents storm translational speeds and a, b, and c are constants. The constant 'c' was scaled such that the value of 'y' is returned in units of percent of cases for 1-knot centered class intervals along the x-axis. For example, entering the equation with an x-value of 5.5 knots will yield an area (probability) of 3.26% for speeds 5 through 6 knots while entering the equation with an x-value of 10.5 knots (near the modal value) will yield an area (probability) of 7.75% for speeds 10 to 11 knots. Summing these individual class-interval probabilities over the domain of the distribution will yield a total probability (area) of 100%.

Assuming the availability of at least a hand-calculator, the probability of any range of speeds can easily be obtained. For example, it can be shown that the probability of storms passing San Juan with speeds exceeding 20 knots is about 11.6%. Here, the integration is performed from centered class-intervals from 0.5 to 19.5 knots and the resultant area (88.4%) subtracted from 100%. Similarly, it can be shown that the probability of storm translational speeds exceeding 30 knots is only 0.6%. These same results can graphically be obtained directly from Chart 12.

6.12.2.2 Parameter estimation - The constants "a" and "b" are often referred to as "shape" and "scale" parameters of the distribution. There are various ways of solving for these constants, a discussion of which is beyond the scope of this manual. A simple "moment-estimate" method is used in HURISK.

Crutcher and Joiner (1978, 1980), who use a slightly different form of the Gamma distribution than the one used in HURISK, point out that moment-estimates (as well as other estimates) of the shape parameter are apt to be too large for small sample sizes. The authors recommend the application of a bias reduction factor whenever the sample size drops to below 30 and this recommendation was incorporated into the HURISK algorithm. Small sample sizes occur much more frequently in Chart 13 (where tropical storms are excluded) than they do in Chart 12 (which includes both hurricanes and tropical storms). Application of the bias corrector also prompted a small adjustment to the standard deviation of storm speeds so as to maintain the same mean value.

6.13 CHART 13

6.13.1 Chart Description

Chart 13 (Fig. 13) is identical to Chart 12 except that it deals with hurricanes only whereas Chart 12 includes tropical storms as well. The different shape of the speed distribution from that given in Chart 12 can be noted (see Section 6.13.2, below). A slightly different value of mean storm speeds could occur between Chart 13 and other charts which refer to storm speed (Chart 6, for example). The explanation for this possible difference is given in Section 6.1.3.

GAMMA DISTRIBUTION OF STORM TRANSLATIONAL SPEEDS
(STORM INTENSITY ≥ 64 KTS)

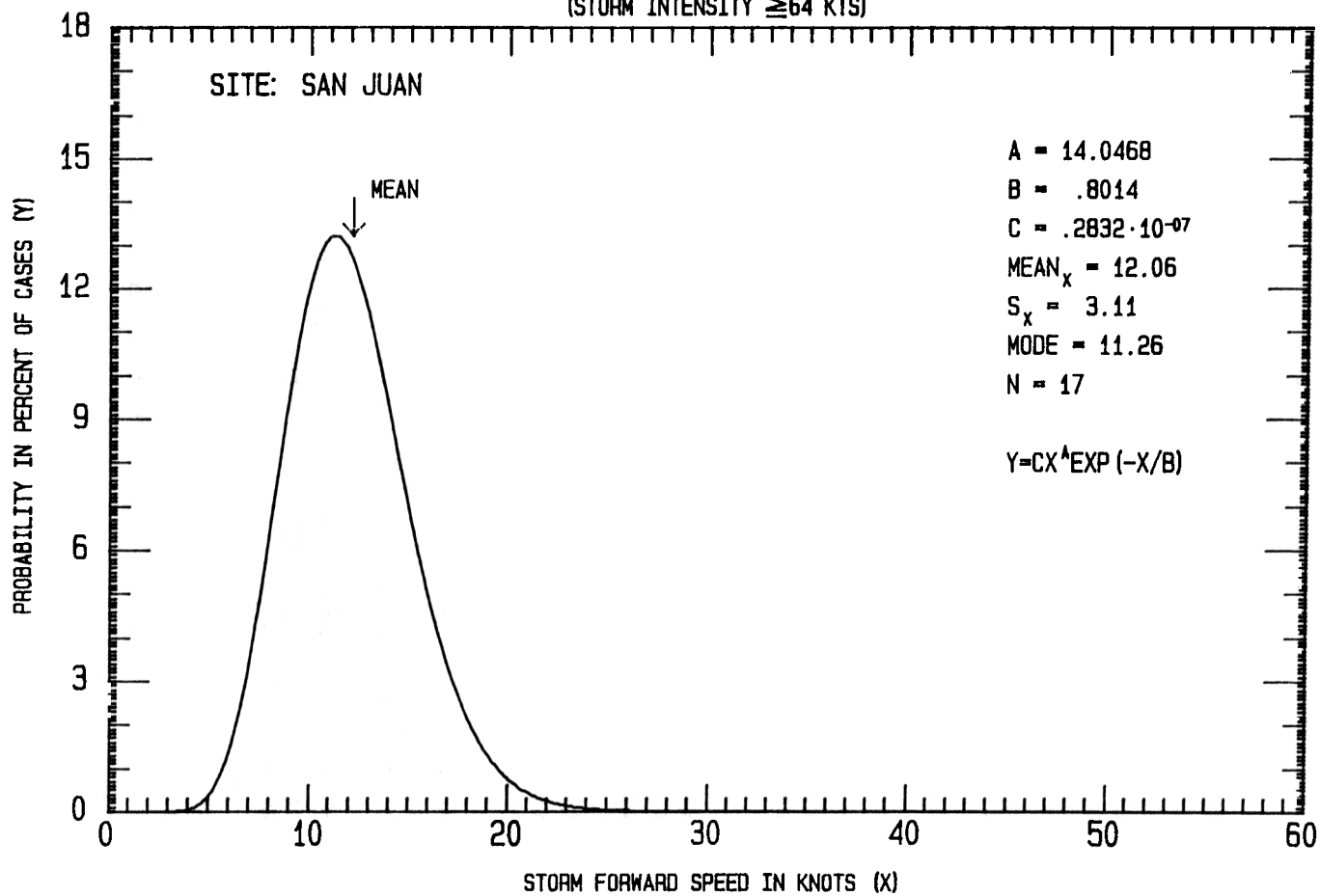


CHART 13

Fig. 13. Same as Fig. 12 except for hurricanes only

6.13.2 Technical Discussion

6.13.2.1 Application of "t-test" - It often happens that the average speeds of hurricanes are different from those of tropical storms. In Chart 12, for example, the mean speed of storms as they pass nearest to the site, is given as 13.2 knots whereas in Chart 13, this value is given as 12.1 knots. The standard deviations, likewise, are different. The question arises as to the statistical significance of these differences. Could they reasonably be expected by chance? Statistically, the "t-test" (Mills, 1955) is often called upon to assess the situation. These t-test computations are included as supplementary rather than graphical output and are available to users.

6.14 CHART 14

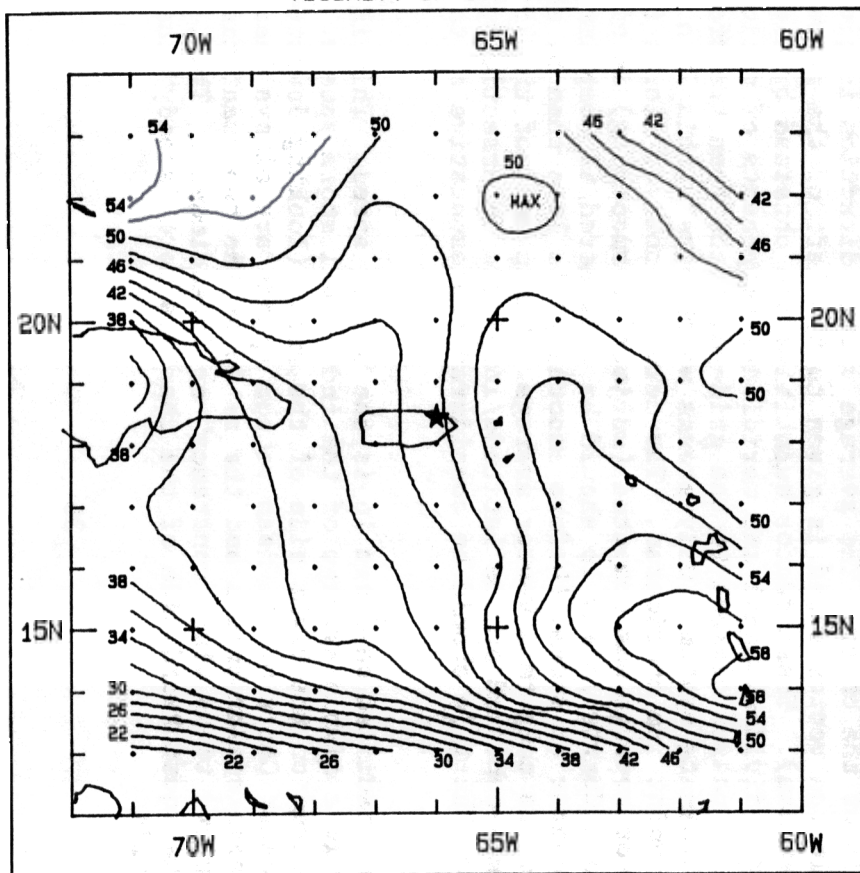
6.14.1 Chart Description

Chart 14 (Fig. 14) is an analysis of storm frequency over a 10 x 10 degree zone centered on the site. The chart is quite useful in assessing the overall tropical cyclone frequency in vicinity of a site and helps to explain inter-site risk differences. The chart presents "isolines" connecting points of equal storm frequency with the latter being defined as the number of storms passing within 75 n.mi. of the site. The analysis example given in Fig. 14, shows storm frequency to be decreasing from east to west across Puerto Rico. Thus, to a degree, the eastern edge of the island would be subject to more tropical cyclone activity than the western edge. In that the intensity of these storms is not considered in this depiction, there may not be a perfect relationship with, say, the gradient of a 50-year storm event over the island of Puerto Rico. That is, the magnitude of a 50-year storm or any n-year storm need not necessarily decrease from east to west in exactly the same manner as suggested by the storm frequency analysis. In this connection, Chart 15, which presents this same type of analysis for hurricanes alone, should also be considered.

The number of storms affecting the San Juan area, as suggested by the analysis, may not agree exactly with the number of storms given elsewhere in HURISK. There are two reasons for this. One concerns the fact that the site location has been adjusted somewhat for storm asymmetry (see Section 6.2.2) and the site location as plotted on the figure is the unadjusted, rather than the adjusted position. The other reason is that the isolines given on Fig. 14 have been smoothed so as to remove any small-scale variations in storm frequency from the analysis.

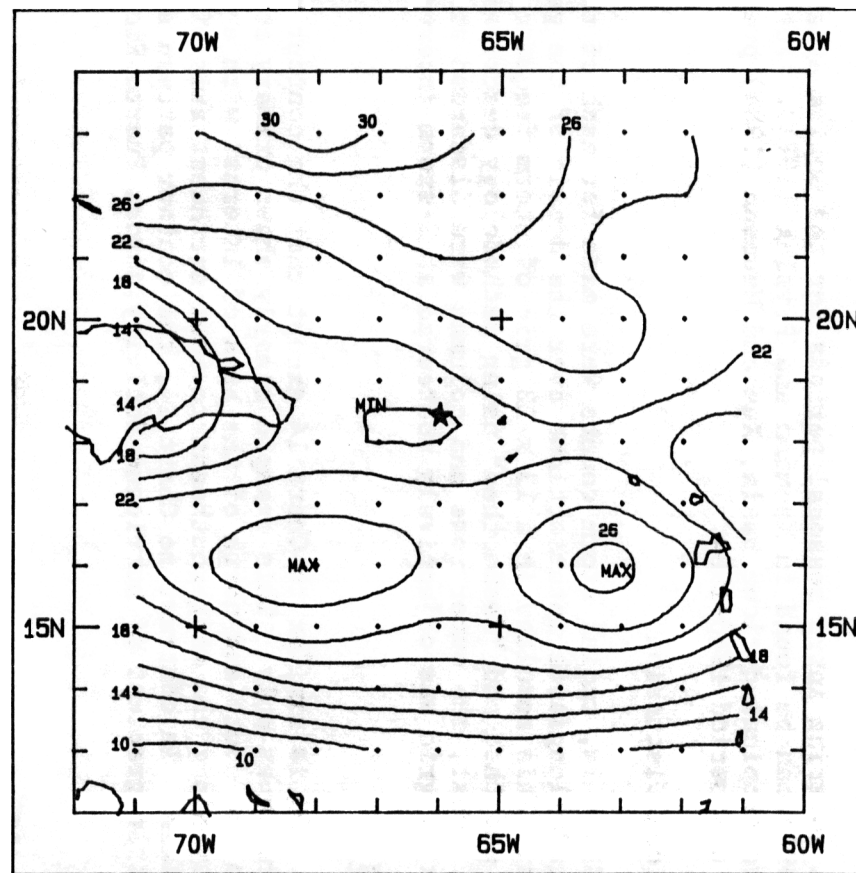
Areas of maximum and minimum storm occurrence (in the relative sense) are also depicted. In this example, a relative maximum appears near 22.0N, 64.5W. This area is flagged since storm frequency decreases outward in every direction from that point. Areas with higher maximum values such as near 14.0N, 61.0W are not flagged since they are not "closed" centers. Insofar as "closed" areas of relative minimum storm frequency are concerned, none appear in this example but do appear on Chart 15 (Fig. 15).

GEOGRAPHICAL DISTRIBUTION OF STORM FREQUENCY IN VICINITY OF SAN JUAN



SOLINES DEPICT NUMBER OF TROPICAL CYCLONES WITH MAXIMUM WINDS OF AT LEAST 34 KNOTS PASSING WITHIN 75 N M OF ANY POINT. 886 1987

GEOGRAPHICAL DISTRIBUTION OF TORNADO FREQUENCY IN VICINITY OF SAN JUAN



ISOLINES DEPICT NUMBER OF TROPICAL CYCLONES WITH MAXIMUM WINDS OF AT LEAST 64 KNOTS PASSING WITHIN 75 N M OF ANY POINT. 886 1987

Similar charts covering intra-seasonal periods for the entire Atlantic basin (1886-1980) can be found in Neumann and Prysak (1981). For the Western Pacific tropical cyclone basin, Xue and Neumann (1984) present such data for the period 1946-1984.

6.14.2 Technical Discussion

In preparing Chart 14, radial storm counts were made for each of the 1-degree latitude/longitude intersections over the domain of the geographical area. This resulted in a 13 x 13 grid of storm frequency. The data were smoothed and "desmoothed" using methodology described by Shuman (1957). Next, the outer rows and columns were discarded and the resulting 11 x 11 grid was objectively contoured at 2-storm intervals.

CHART 15

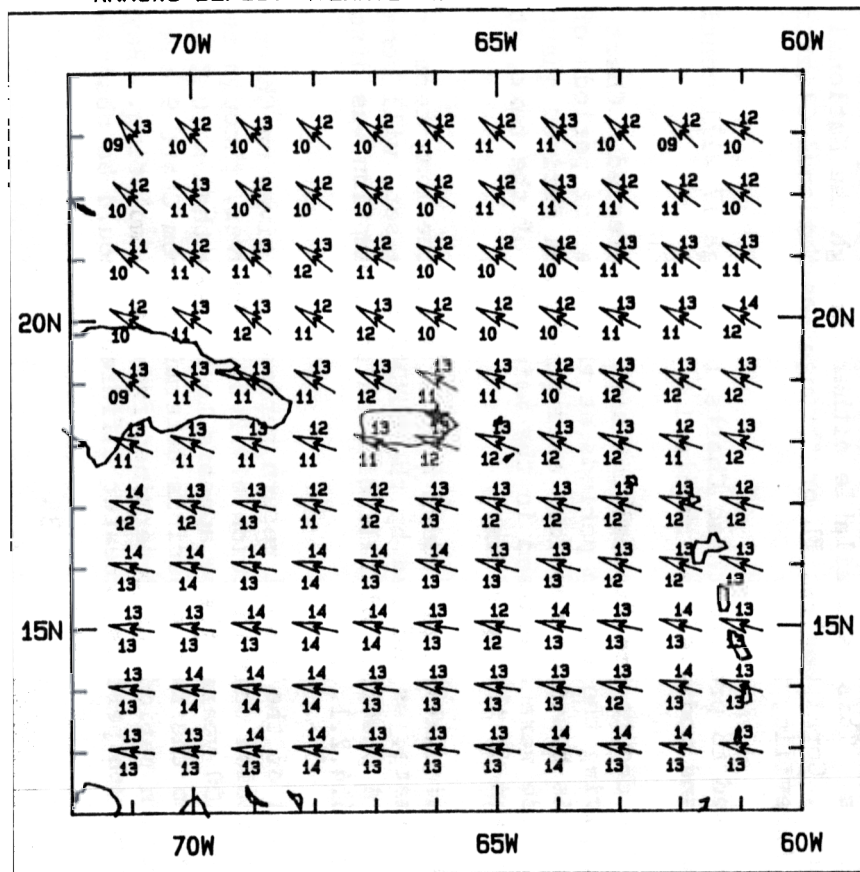
Chart 15 (Fig. 15) is similar to Chart 14 except that the contour analysis is for hurricanes only. This example clearly shows primary storm tracks both to the south and north of the area of interest with a minimum of activity along the east-southeast to west-northwest axis of the main island chain. In contrast to Chart 14, the contour pattern suggests very little gradient of hurricane activity across Puerto Rico.

CHART 16

Chart 16 (Fig. 16) is a depiction of the geographical variation of storm motion characteristics over a reasonably large area around the site. Three items are specified for each of the 11 x 11 = 121 grid points (which are positioned at the 1-degree latitude/longitude intersections) over the domain of the chart. The average vector direction is given by the arrow while the vector speed is given to the left of the arrow (looking downstream). These vector quantities are obtained by algebraically summing individual zonal and meridional components of motion for each storm as it passes closest to the grid-point and then transforming to a polar coordinate system. Only storms which pass within 75 n.mi. from the grid-point are considered. The actual number of storms from which the vector average was computed (subject to smoothing) is given in Chart 14. Thus, Charts 14 and 16 should be considered as complimentary. If the total number of storms (before smoothing) is less than 5, no attempt is made to compute a vector average. Since each of the 75 n.mi. scan-circles was centered at the latitude/longitude intersections, the values given on Chart 16 should be considered representative at that point.

The third item specified on Chart 16 is the scalar speed. This is obtained through a simple average of the individual storm speeds. These speeds are entered on the right side of the arrow (looking downstream). As discussed under Chart 6, the mean vector speeds are always less or equal to the mean scalar speeds and the ratio of the two quantities is sometimes referred to as wind "constancy" or "steadiness". Thus, storm motion over the equatorward side of the chart is more "steady" than over the poleward side.

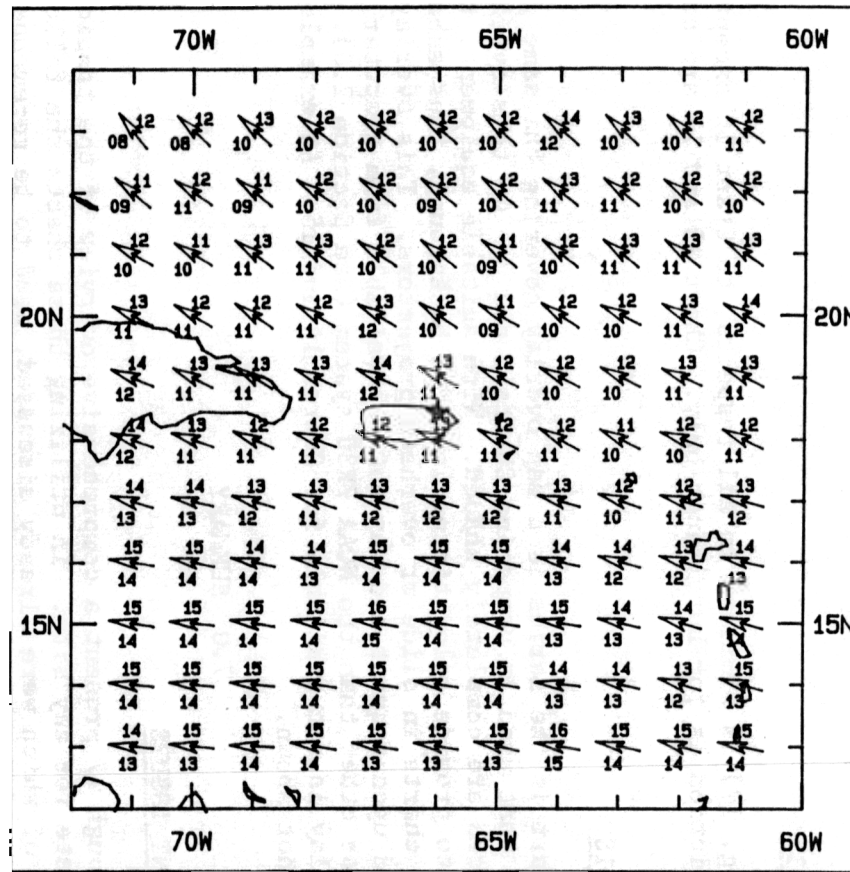
TROPICAL STORM & HURRICANE MOTION (1886-1987) NEAR SAN JUAN
ARROWS DEPICT AVERAGE VECTOR HEADING OF STORMS



NUMBERS ADJACENT TO DIRECTION ARROWS GIVE AVERAGE VECTOR AND SCALAR STORM SPEEDS IN KNOTS. VECTOR SPEEDS ARE \leq SCALAR SPEEDS. ASTERISK (*) INDICATES < 5 STORMS.

CHART 16

HURRICANE MOTION (1886-1987) NEAR SAN JUAN
ARROWS DEPICT AVERAGE VECTOR HEADING OF STORMS



NUMBERS ADJACENT TO DIRECTION ARROWS GIVE AVERAGE VECTOR AND SCALAR STORM SPEEDS IN KNOTS. VECTOR SPEEDS ARE \leq SCALAR SPEEDS. ASTERISK (*) INDICATES < 5 STORMS.

CHART 17

Fig. 16. Variation of tropical storm and hurricane motion in vicinity of site (CHART 16).

Fig. 17. Variation of hurricane motion in vicinity of site (CHART 17).

6.17 CHART 17

Chart 17 (Fig. 17) is similar, in all respects, to Chart 16 except that the depiction is for hurricanes only. Chart 15 and 17 are complementary.

6.18 CHART 18

The final chart in the series is a map overlay covering the same geographical area as that used in preparing Charts 2 and 3. On this overlay, the land masses are completely shaded. With suitable equipment, this can be used to provide color-tinted landmass background, thus enhancing use of these charts in slide or overhead projectors. This overlay is only included upon request and may not be available from computer plotter facilities other than the NOAA FR80 system (see Section 2.0). A similar overlay is not available for Charts 14 and 15. An example of Chart 18 is not shown.

7.0 SUMMARY

IMPORTANT ISSUES

Charts 1 through 17 present a comprehensive overview of the tropical cyclone climate for any site. In utilizing these charts the following points, most of which were already discussed, need to be re-emphasized.

- (1) A supplemental publication, "Tropical Cyclones of the North Atlantic Ocean: 1871-1986" (Neumann et al. 1987) is highly recommended for additional background information on various aspects of tropical cyclones. This is available either through the National Hurricane Center, Coral Gables, FL or through the National Climatic Data Center, Asheville, NC.

The data used to prepare these Charts 1 through 17 will continually be updated and modified, as required.

- (3) Most of the charts are factual but some are inferred. Chart 9, for example, giving the return periods at the site for periods of up to 450 years, is based on numerous assumptions and derived quantities. Some of these were discussed in the main body of the text, others are discussed in the Appendix.
- (4) The entire simulation procedure assumes that the long-term tropical cyclone climate, as defined by the HURDAT data set, will remain unchanged. A possible pitfall of such an assumption was discussed in Section 6.4.2.1.

The position of the dashed return period line given on Chart 9 is an approximation only (Section 6.9.2.3). However, through return periods of 100 years, there appears to be less than a 10 % difference between the return periods determined from Chart 9 and the "true" return periods as determined from the simulation. Beyond 100-year return periods, greater differences could be observed.

- (6) Before making profound decisions from these data, users should seek further meteorological and statistical advice.
- (7) A qualitative assessment on the confidence of the return period simulations is given at the end of the Appendix.
- (8) If a risk analysis is to be performed (Chart 9), the scan-circle radius must be set at 75 n.mi.

7.2 REQUEST FOR USER COMMENTS

User comments, as to the adequacy, arrangement, contents, utility, understanding, etc. of the various Charts, are welcome. Forward any comments to the National Hurricane Center, 1320 South Dixie Highway, Coral Gables, FL 33146.

APPENDIX A

PURPOSE

The main body of the text contains descriptions of the various graphs and charts produced by the HURISK program. Although some technical discussion was given, the main technical issue, that is, the return period computations, was reserved for this supplement. To foster better understanding of the overall procedure, a flow-chart, covering the highlights of the computer simulation procedure, is presented as Fig. A-1. Frequent reference will be made to this schematic diagram.

BACKGROUND

The term "Monte-Carlo simulation" usually refers to the use of a computer random number generator to simulate some of the random processes found in the universe. It is often used, as it is here, to find empirical solutions to rather complex mathematical problems. (Hamming, 1962, Tsokos, 1972). In relation to the generation of tropical cyclones parameters, the methodology was first described by Russell (1971) and later applied and refined by other researchers in this field such as Batts, et al, (1980), Georgiou et al. (1983) and Georgiou (1985). The latter, a PhD thesis, gives a particularly thorough treatment of the subject.

Some of the procedures used in HURISK are similar to those used by the other authors; others are not. Basically, the various parameters which contribute to tropical cyclone induced winds are fitted to parent probability distributions or functions using historical records. It is also necessary to determine the inter-correlations between the various parameters. For an individual simulation, the computer selects from each of these distributions separately and then combines them in a logical manner after taking the inter-correlations into account. One rarely finds, for example, a large radius of maximum wind with an intense storm. It is very important that these parameter relationships be properly maintained throughout the simulation and it is in this area that individual researchers often differ in their methodology (and results).

The HURISK procedure for determining tropical cyclone return periods is somewhat less complex than used by other authors. It does not attempt to simulate the direction of the wind, only the speed. Another difference between HURISK and other procedures is that it makes rather explicit use of tropical cyclone winds as recorded on the HURDAT (Jarvinen et al. 1984) data set. Also, HURISK treats the problem of wind asymmetries quite differently than other researchers in this field. In essence, HURISK was designed to provide a reasonable estimate of wind return periods through about 100 years. One distinct advantage of HURISK over other procedures is the provision for providing enough background material to allow a subjective evaluation of the objective return period calculations.

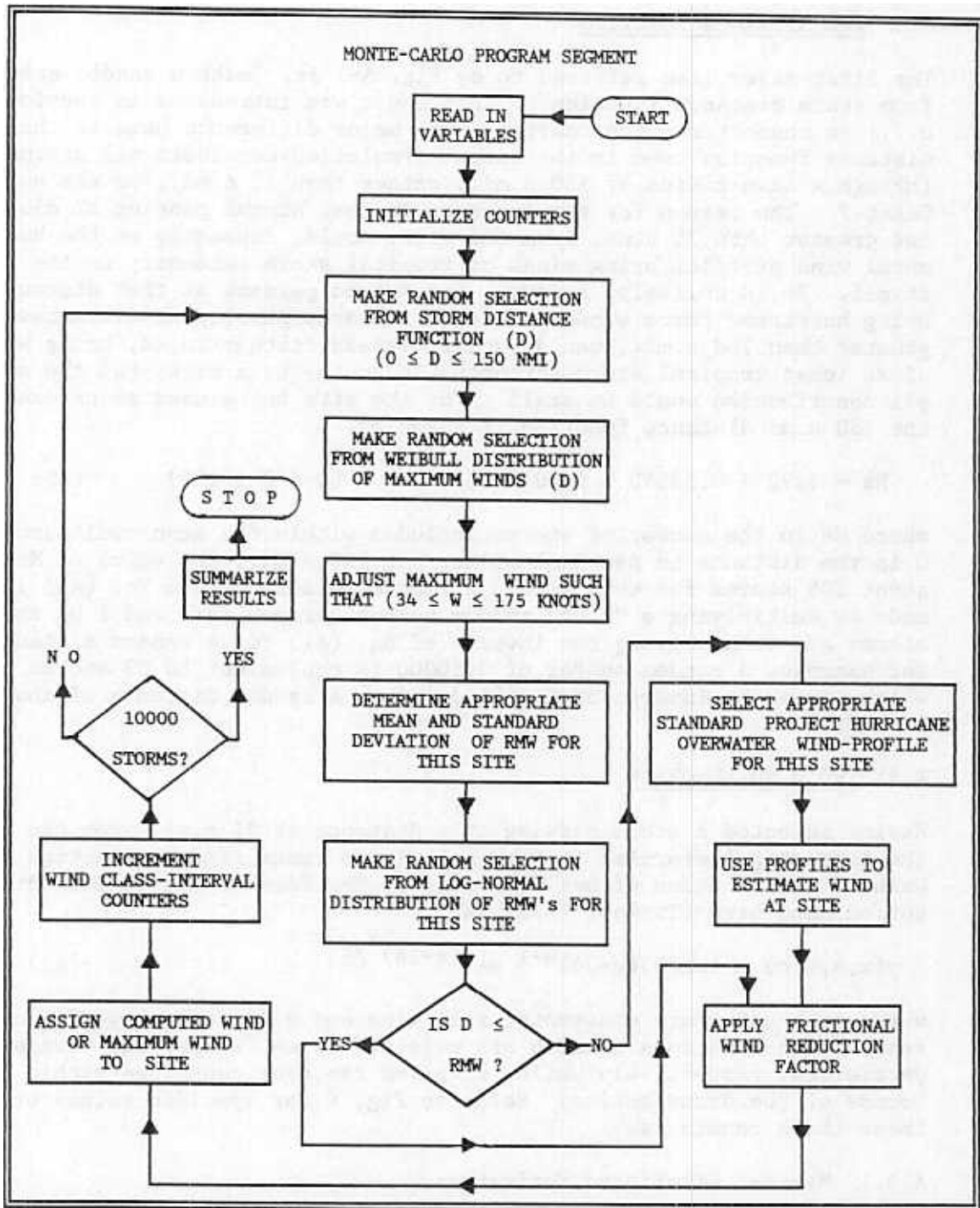


Fig. A-1. Monte-Carlo program segment

A.3 THE DISTANCE FUNCTION

The first major item referred to on Fig. A-1 is, "make a random selection from storm distance function". This topic was introduced in section 6.7.1 in connection with Chart 7. One major difference here is that the distance function used in the actual simulation considers all storms out through a scan-radius of 150 n.mi., rather than 75 n.mi., as was used in Chart 7. The reason for the increase is that storms passing at distances greater than 75 n.mi. from the site, could, depending on the horizontal wind profile, bring winds of tropical storm intensity to the site itself. It is unlikely, however, for storms passing at that distance to bring hurricane force winds to a site. Storms passing at distances greater than 150 n.mi., could, under certain circumstances, bring winds of at least tropical storm strength (34 knots) to a site, but the overall contribution would be small. For the site being used as an example, the 150 n.mi distance function is given by,

$$N_s = 3.22 + 0.5354D + 0.00100D^2 \quad (0 \leq D \leq 150) \quad (A1)$$

where N_s is the number of storms included within the scan-radii area and D is the distance in nautical miles. At 150 n.mi., the value of N_s is about 106 storms for this site. A random selection from Eq. (A1) is made by multiplying a "flat" random number between zero and 1 by the 106 storms and then solving the inverse of Eq. (A1) for a random distance. For example, a random number of 0.50000 is equivalent to 53 storms which, from the inverse of Eq. (A1), gives a random distance of about 81 n.mi.

A.4 THE WIND FUNCTION

Having selected a storm passing at a distance of 81 n.mi. from the site, the next step (referring to Fig. A-1) is to "make random selection from Weibull distribution of maximum winds". The form of the Weibull distribution used here (Tsokos, 1972) is,

$$y(x,a,b,c) = (ca/b)(x-34)^{a-1} e^{[-(x-34)^a/b]} \quad (A2)$$

where a , b and c are constants, x is wind and y is frequency of occurrence. The constants a and b are referred to as "shape" and "scale" parameters, respectively while ' c ' gives the area contained within the bounds of the distribution. Refer to Fig. 8 for specific values of these three constants.

A.4.1 Maximum Likelihood Estimators

There are various methods for estimating values of the shape and scale parameters and the method of maximum likelihood is typically used. The method (and the computer source code) to estimate these parameters is given by Abernethy et al. (1983). The shape parameter ' a ', through iteration, is found by satisfying the following equation where x_i through x_n are the 43 values of maximum wind given in Fig. 1, Column 7:

$$\frac{\sum_{i=1}^n [(x_i)^a \ln(x_i)]}{\sum_{i=1}^n (x_i)^a} - \frac{1}{n} \sum_{i=1}^n \ln(x_i) - 1/a = 0$$

Having found an estimate of the shape parameter 'a' from Eq. (A3), the estimate of scale parameter 'b' is obtained from,

$$b = \frac{\sum_{i=1}^n (x_i)^a}{n}.$$

Equation (A4) has been slightly modified from that given in the previously cited reference so as to be consistent with the form of the Weibull distribution used in HURISK.

A.4.2 Random Selection from Weibull Distribution

A random selection of maximum wind (W_{\max}) from Eq. (A2) is made from (Hahn and Shapiro, 1967; Abernethy, et al. 1983),

$$W_{\max} = [b \ln(1/1-R_f)]^{1/a} + 34$$

where R_f is a selection from a flat random number distribution ($0 \leq R_f \leq 1$). For example, using the values of 'a' and 'b' given on Fig. 8 and a random number of 0.75000, a W_{\max} of about 68 knots is computed from Eq. (A5). At this point, a storm, having a maximum sustained 1-minute wind of 68 knots, is passing at a closest-point-of-approach to the site of 81 n.mi.

A.4.3 Adjustment of R_f in Eq. (A5)

In the main body of the text (Section 6.9.2.2), the issue concerning maximum possible intensity of hurricanes was discussed and it was pointed out that 175 knots was chosen as a reasonable maximum. From the inverse of Eq. (A5), this is equivalent to an R_f of about 0.99304 in this example. Accordingly, all values of R_f were multiplied by 0.99304 such that the maximum possible value of W_{\max} from Eq. (A5) would be 175 knots.

Clearly, truncation methodology is an exceedingly important issue since it directly effects the estimates of long-term return periods. More realistic methods of accomplishing this are being sought and it is likely that modifications to the algorithm will be made in this area. Ideally, any constraint to W_{\max} should duplicate the natural process insofar as possible.

A.5 RADIUS OF MAXIMUM WIND (RMW)

Continuing through the flowchart shown in Fig. A-1, the next boxed item is, "determine appropriate mean and standard deviation of RMW for this site". Conceptually, RMW is simply the radial distance outward from the center of storm circulation ("eye") where the winds reach a maximum value. This typically occurs a few miles radially outward from the eye-wall. Realistically, however, the concept is not so simple and statistical modeling of RMW is fraught with difficulty. Some of the problems are:

- (1) RMW is correlated with some of the other parameters used in the HURISK model. Therefore, random selection of RMW must be qualified.
- (2) A precise measurement of RMW is often not possible in a given storm.
- (3) RMW may vary from one storm quadrant to another.
- (4) There may be multiple, itinerant RMW's.
- (5) Long-term documentation of RMW, taken simultaneously with other parameters, is not available.

Much more could be said about the above listed problem areas and the interested reader is referred to Georgiou (1985) for a complete review and list of pertinent references. Also, Willoughby et al. (1982) focus attention on item (4), above. Additional background information is provided by Shea and Gray (1972).

A.5.1 RMW methodology used in HURISK

The RMW issue is so mired in uncertainty that the decision was made to re-examine some of the basic raw data. Unfortunately, long-term records of RMW, similar in concept to the HURDAT data-set (Jarvinen et al. 1984) are not available. Part of the problem here is certainly related to the tenuity of RMW.

The National Weather Service (NWS) Office of Hydrology has, mainly in connection with the NWS storm-surge program, conducted a large amount of R&D in this area and many of their publications contain data on RMW, principally in regard to hurricanes crossing the United States coastline. Three of these publications (Schwerdt et al. 1979; Ho, 1975 and Ho et al. 1987) were used to obtain 208 measurements or computations of RMW along with storm latitude and intensity. These latter two parameters (and perhaps, others) are correlated with RMW. Because of the scarcity of readily available and reliable RMW data in the deep tropics, it was necessary to include some data from the Western Pacific (south of 18N) and 41 of the 208 cases are from that basin. These data were used to establish relationships between RMW, standard deviation of RMW, latitude and storm intensity.

A.5.1.1 Pressure-wind relationships - Most of the Office of Hydrology storm-intensity data are in terms of central-pressure and it was necessary to establish a relationship between central-pressure and 1-minute sustained wind for use in HURISK. As discussed earlier, HURISK storm intensities are based on the long-term records of wind contained in the HURDAT data-set (Jarvinen et al. 1984). In the past, much work has been focused on this relationship and regression equations which statistically couple the two quantities are available. In connection with HURISK, the wind-pressure relationship was re-examined using the 3276 simultaneous pressure and wind values given in the HURDAT data set through 1986 excluding the extratropical and sub-tropical stages, if any, of storms. The following relationship was found,

$$W = -4032.1 + 9.95p - 0.00588p^2 \quad (A6)$$

where W is 1-minute average wind in knots and p is pressure in millibars. The correlation coefficient associated with the fit is $R_m = 0.997$. However, this value is inflated due to the method of computation. Average pressures were computed for 5-knot wind-bands and these, in turn, were fitted to a second-order polynomial. The inflated value of R_m is due to an artificial constraint in standard deviation using this local-fitting procedure. An adjusted correlation would be more in the order of 0.85. The rationale for fitting locally to the data rather than over the data set as a whole, is that a better fit is obtained in the region of extreme winds where the sample size diminishes. This is an important consideration in the context of HURISK. A graph of the function is given as Fig. A-2. Eq. (A6) is not recommended for purposes other than HURISK.

A.5.1.2 RMW/maximum wind/latitude relationships - The 208 cases of radius of maximum wind (dependent variable), storm latitude and storm intensity (independent variables) were subjected to a multiple regression analysis allowing potential predictors through the 3rd-order products and cross-products of the independent variables. Initially, considering only first-order variables, it was found that there was a statistically significant relationship between dependent and independent variables in the sense that RMW, on the average, is directly proportional to latitude and inversely proportional to storm intensity. However the relationship of

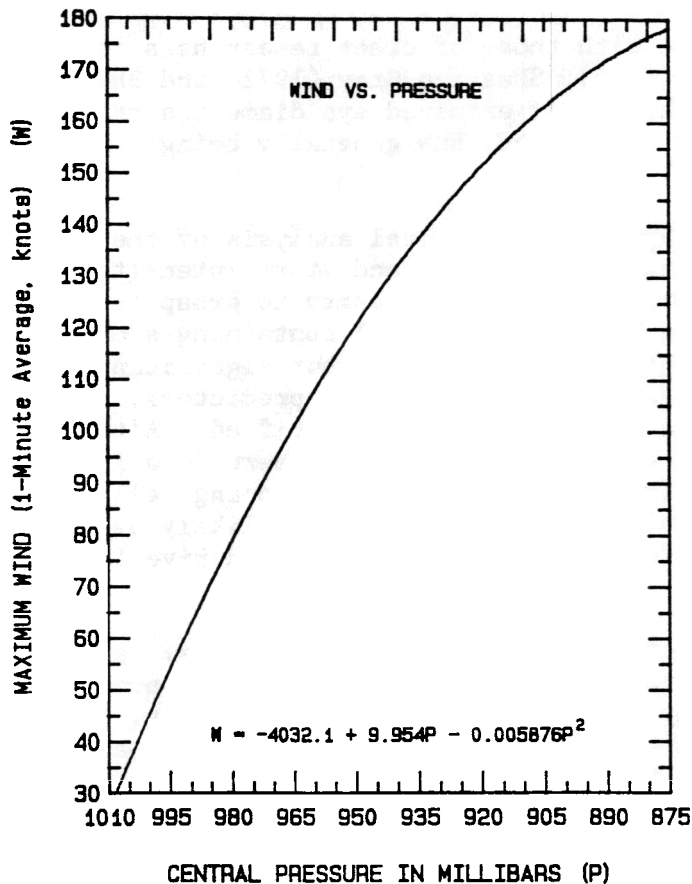


Fig. A-2.

Maximum wind as an empirically derived function of storm central pressure

RMW with latitude is much stronger than with storm intensity. The multiple correlation coefficient of the fit was 0.64; the linear correlation between RMW vs. latitude and RMW vs. storm intensity are 0.61 and -0.32, respectively. However, once the effects of correlation between latitude and storm intensity have been accounted for, the partial correlation coefficient between RMW and intensity drops to -0.23, a level which is barely significant at the 99% level. However, further investigation showed that the latter relationship improved considerably if only intense storms (over 100 knots) were included in the analysis. Since this is important in the context of HURISK, the decision was made to retain intensity in the regression equation.

The form of the equation finally adopted is shown in Fig. A-3 and the three basic findings discussed in the preceding paragraph can be noted in the plot:

- (1) RMW is directly proportional to latitude and inversely proportional to storm intensity.
- (2) The effect of latitude on RMW is greater than the effect of storm intensity.
- (3) The inverse relationship between RMW and storm intensity increases rather rapidly with increasing storm intensity.

These results agree in principle with those of other researchers including Ho et al. (1987), Georgiou (1984), Shea and Gray (1972) and Sheets (1972). In the latter study, the author examined eye diameters rather than RMW but the two are highly correlated, RMW generally being a few miles larger than eye radius.

A.5.1.3 Standard deviation of RMW - A statistical analysis of the standard deviation of RMW as a function of latitude and storm intensity was also accomplished. For this purpose, it was necessary to group the data into two-dimensional overlapping "cells", each cell containing about 20 cases. The resulting relationship was rather weak, but significant, in the statistical sense. The inclusion of higher order predictors, as was accomplished in the case of mean RMW, could not be justified. Although the actual multiple correlation coefficient was 0.82, there is a large and unknown loss in degrees-of-freedom using the overlapping cell methodology such that an adjusted multiple correlation would likely be considerably lower than 0.82. No formal attempt was made to derive this value.

The adopted relationship and plot are given in Fig. A-4. Thus, standard deviation of RMW, similar to the mean of RMW, is directly proportional to latitude and inversely proportional to storm intensity. The study by Sheets, referred to in the preceding paragraph, and on a completely different data set than that used in HURISK, suggests a similar relationship.

A.6 LOG-NORMAL DISTRIBUTIONS OF RMW

The next entry in the program segment shown in Fig. A-1 is, "make random selection from log-normal distributions of RMW's for this site". Choice of this particular distribution was prompted by the work of other auth-

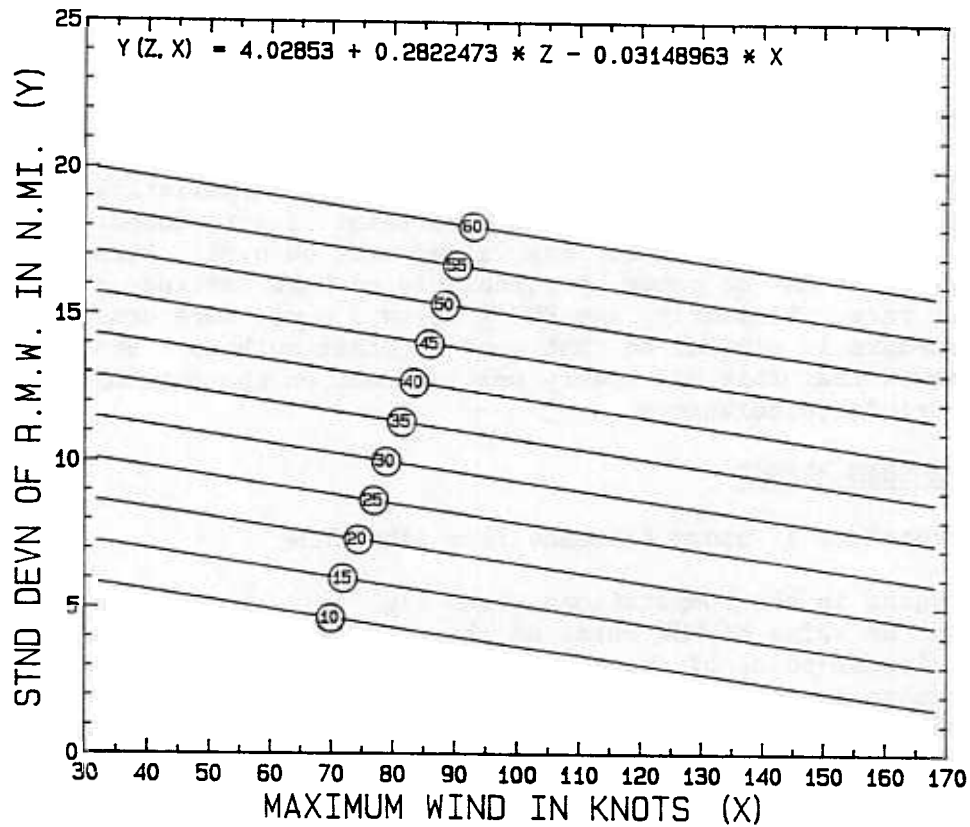
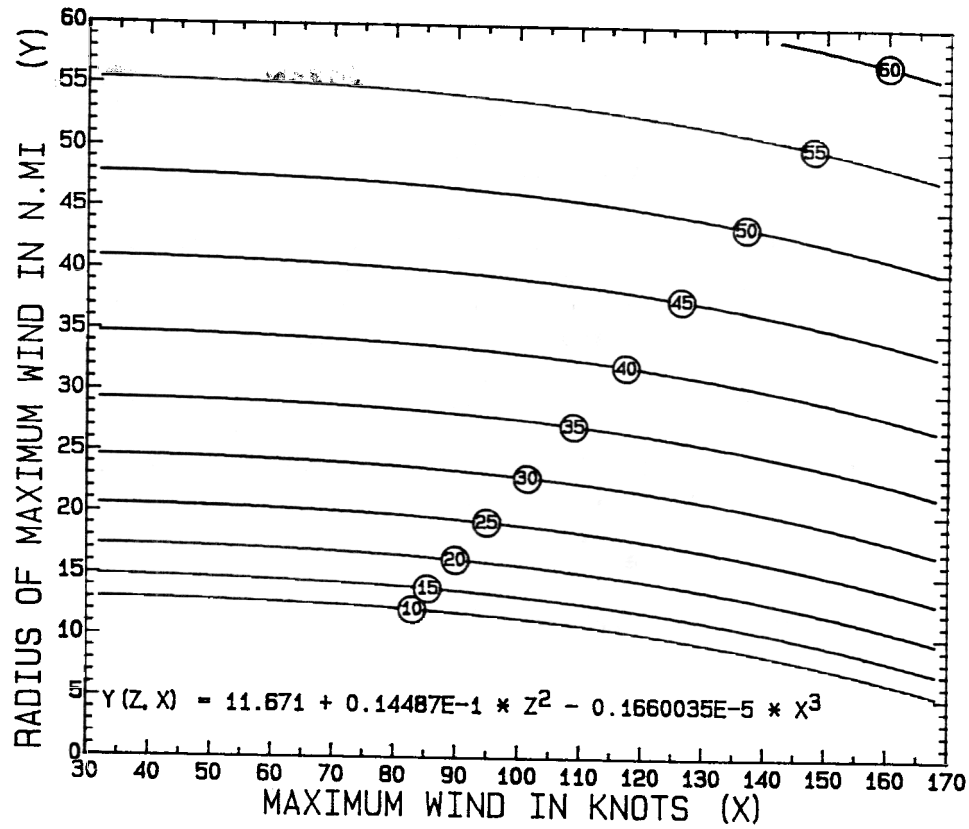


Fig. A-3. (TOP) and Fig. A-4. (BOTTOM) give, respectively, mean and standard deviation of radius of maximum wind as empirically derived functions of storm maximum wind and storm latitude (z, circled).

ors, notably, Batts, et al. 1980 and Georgiou (1985). The distribution is given (Hahn and Shapiro, 1967) by,

$$y(x) = 1/(ax\sqrt{2\pi}) e^{-[1/(2a^2)][\ln(x)-b]^2} \quad (A7)$$

where 'a' (shape parameter) and 'b' (scale parameter) are constants, 'x' is RMW and 'y' is frequency. The two constants are estimated by moment estimates using the mean (m) and standard deviation (s) as obtained from the equations given on Figs. A-3 and A-4, respectively,

$$m = e^{2b + \frac{1}{2}a^2}, \quad s^2 = e^{2b + a^2}(e^{a^2} - 1). \quad (A8)$$

Finally, a random selection (y') from the distribution described by A7 and A8 is obtained from,

$$y' = e^{aR' + b}, \quad (A9)$$

where R' is a random selection from a normal distribution having mean zero and standard deviation, 1.0. This is to be distinguished from earlier random selections (R_f) from "flat" distributions between zero and 1.0.

Examples of these randomly generated distributions are shown in Fig. A-5. The lower two distributions are for the latitude of the site being used as an example while the upper two distributions are for the latitude of Atlantic City, NJ. The attributes of these examples are, of course, in agreement with those given on Figs. A-3 and A-4.

A.6.1 Truncation of distributions

Eq. (A7) is unbounded at the upper end such that unrealistically large RMW's could be obtained unless some constraint is introduced. The constraint used here is to censor any values over 60 n.mi. Although such large values of RMW do occur, particularly on high latitude storms, they are quite rare. Similarly, any RMW's below 3 n.mi. were censored. This procedure is similar to that used by other authors. Sensitivity tests showed that this had a very small effect on the outcome of the return periods calculations.

A.7 A PROGRAM BRANCH

A.7.1 Procedure if storm distance from site \leq RMW

At this point in the computations, (see Fig. A-1), a decision is made in regard to the value of RMW obtained above and an earlier random selection of closest-point of storm approach described in section A.3. If this distance is less than RMW, there is no need for further calculations and the maximum wind, as determined from an earlier random selection, described in Section A.4, is assigned to the site after applying a frictional wind-reduction factor (see Section A.9). The simplified procedure for addressing asymmetries in the wind circulation was described in the main body of the text (Section 6.2.2).

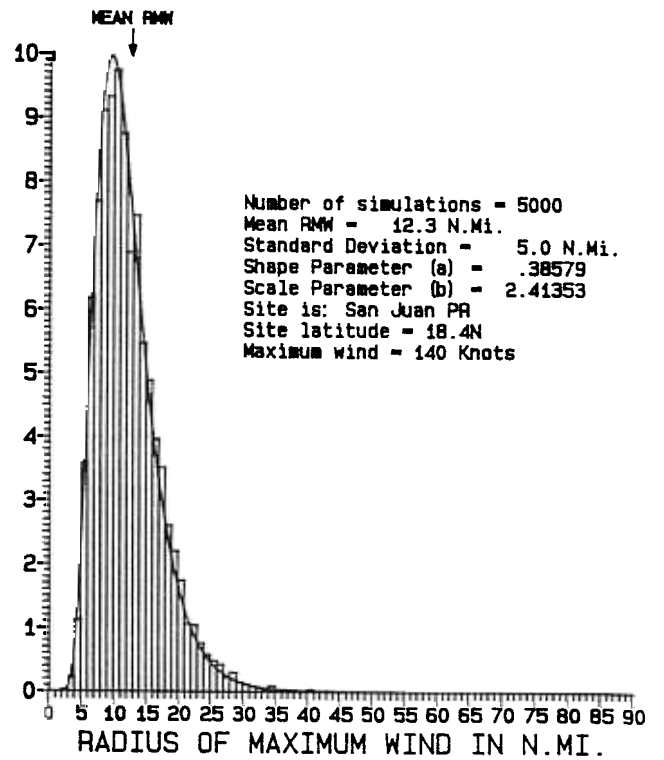
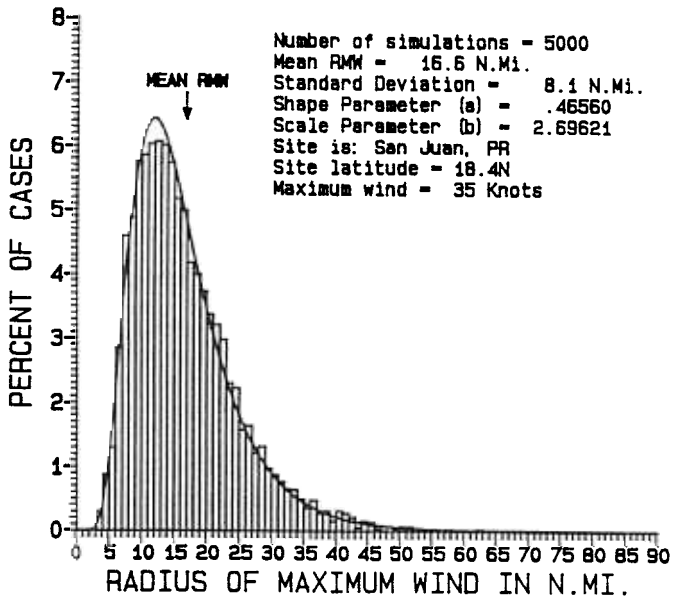
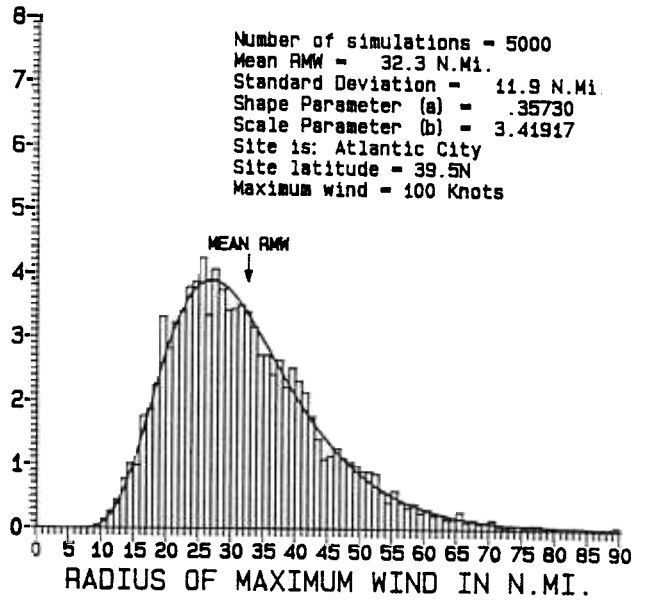
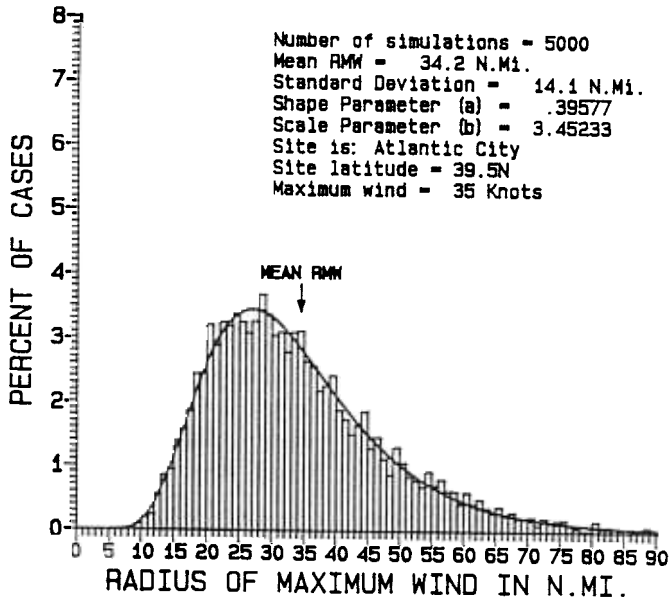


Fig. A-5. Examples of radius of maximum wind (RMW) simulations for two sites and two wind maxima. Each chart shows 5000 simulations from log-normal distribution having specified mean and standard deviation.

Procedure if storm distance from site >RMW

If the closest-point-of-approach is outside the bounds of RMW, further processing is needed to determine an appropriate wind-profile to be used for this situation. This is discussed in Section A.8, below.

HORIZONTAL (STANDARDIZED) WIND-PROFILES

Another relationship that must be addressed at this point is between RMW and the horizontal wind profile. Although there is considerable variation, small and intense tropical cyclones tend to have steep horizontal wind profiles; that is, winds rapidly diminish radially outward from RMW. Failure to account for this condition, even though the overall correlation between RMW and "large" and "small" tropical cyclones is probably rather low, could have a profound effect on return period calculations. The reader is referred to Shea and Gray (1973) and to Merrill (1982) for additional background information.

The profiles used in HURISK were derived by Schwerdt et al. 1979 and are referred to as standard project hurricane (SPH) or probable maximum hurricane (PMH) profiles. These are empirically derived profiles as given on page 27 of the above cited reference. The authors give profiles through a radial distance of 300 n.mi. for RMW values of 4, 6, 10, 15, 20, 30, 40 and 50 n.mi. Since it was difficult to precisely fit these in the mathematical sense, they were digitized for use in HURISK. A method described by Akima (1986) was used for interpolation of intermediate values and extrapolation to the maximum allowable RMW of 60 n.mi. and the minimum allowable RMW of 3 n.mi.

A.8.1 Application of profiles

The profiles, as digitized for HURISK are displayed in Fig. A-6. These profiles yield a ratio of site wind (before any frictional wind reduction) to maximum wind at the storm center for the given distance and for the given RMW. These are "over-water" profiles and the wind derived therefrom must be reduced for frictional effects over land. These effects are discussed in the following section.

FRICTIONAL EFFECTS

A.9.1 Over-water to Over-land Wind Reduction

Referring again to Fig. A-1, the last major step in the return period calculations is accounting for surface frictional influences. The wind-profiles referred to in the previous section are "over-water" profiles. HURISK is designed primarily for use over coastal and near-coastal areas and the wind obtained from Fig. A-6 must be reduced accordingly.

Frictional reduction of wind is probably the most subjective portion of the HURISK procedures. After considerable testing, a friction function patterned after that given by Myers (1954) was adopted [see page 267 of Schwerdt et al. 1979 (NWS 23)]. In this function, the amount of frictional reduction is dependent on windspeed with low wind speeds being decreased considerably more (in the percentage sense) than high wind speeds. In regard to the latter, (above 110 knots), the Myers function,

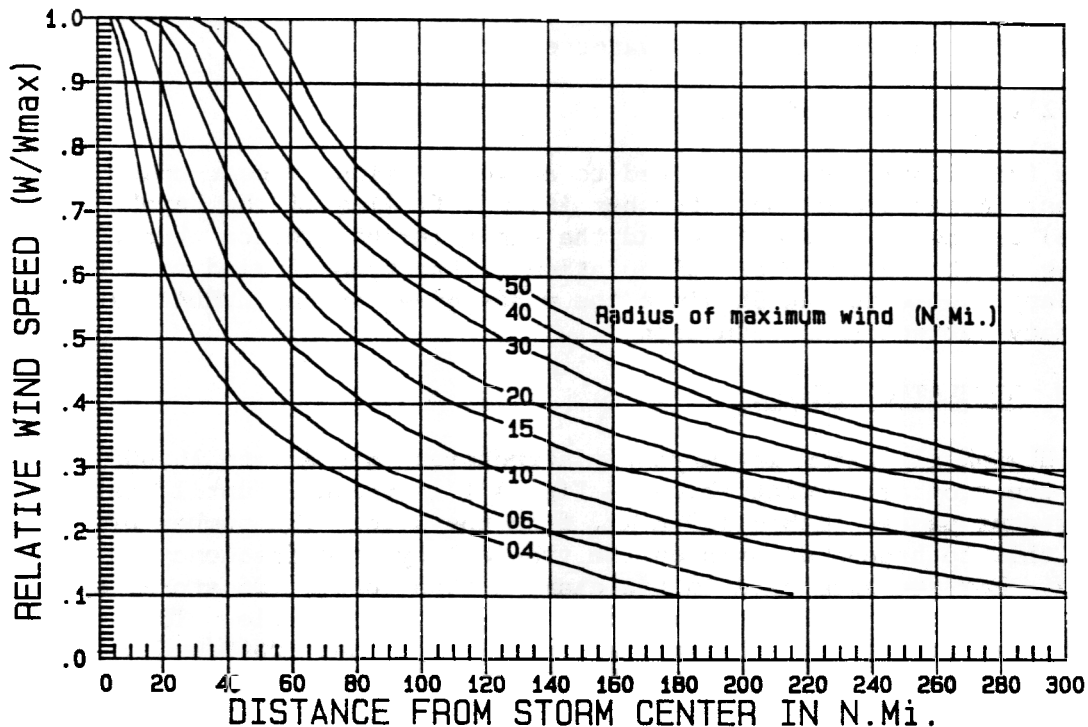


Fig. A-6. Over-water wind profiles (for stationary storms) used in HURISK to obtain wind (W) at specified distances from storm center as a function of radius of maximum wind. W_{max} refers to maximum wind near storm center. These winds are subject to frictional reduction (see text). Profiles are from Schwerdt et al. (1979).

as given by Schwerdt et al. (1979), decreases winds only about 10%. However, numerous experimental HURISK runs suggested that this was somewhat small. Accordingly, a value of about 20% reduction (ratio of 0.80), as suggested in NWS 23, was finally used for these higher winds. To avoid a stepwise function, a gradual blending between the Myers value and the NWS 23 recommended value is used in the HURISK procedure.

The frictional factor referred to above does not begin abruptly as storms cross the coast. Rather, there is a distance, extending seaward from the coast, that the frictional reduction begins to take effect. In NWS 23, this distance is given as 10 n.mi. and this was also used in HURISK. Between the coast line and the 10 n.mi. offshore point, NWS 23 recommends a gradual non-linear increase (see NWS 23, page 33). This recommendation was also adopted for use in HURISK.

The full frictional wind reduction, as discussed above, is applied to site winds which were computed from the horizontal wind profiles, as illustrated in Fig. A-6. A reduced frictional wind reduction factor (approximately 25% of the full reduction) is applied to the maximum winds of storms which pass within the radius of maximum wind. This procedure was adopted after considerable testing of the algorithm and is subject to modification after HURISK is activated for a larger number of

sites. In this connection, the frictional wind reduction factors used in HURISK need to be adjusted (reduced) for small insular sites and eliminated entirely for over-water sites.

A.9.2 Inland wind reduction

This frictional factor referred to above pertains to near-coastal locations. After storms move further inland, filling of the "eye" (pressure rise) begins to take effect and the winds further reduce through a weakening of the entire storm circulation. That type of wind reduction is not applicable to HURISK since the winds given on the HURDAT data source already reflect this reduction.

A.10 SIMULATION PERIOD

The HURISK algorithm is currently structured to simulate 10,000 storms and the program segment shown in Fig. A-1 is recycled until that number of storms passes within 150 n.mi. from the site. The number of years for this to happen depends on the tropical cyclone frequency for the area. For the site used in the example (San Juan), 106 storms over the 102 year period of record passed within the scan-circle. That is equivalent to about 1.039 storms per year or about $10000/1.039 = 9622$ years. Thus, the wind events recorded in the simulations are assumed to have taken place over 9622 years and return periods are computed accordingly. For example, the simulations indicated that San Juan will experience at least 100 knot 1-minute sustained wind events on 64 occasions over the next 9,922 years. This is a return period of $9622/64$ or about once every 150 years, on the average. This is slightly different than the 153 year return period of 100-knots winds mentioned in Section 6.9.1.1. The small difference is a result of the simplified procedure actually used in HURISK and discussed in Section 6.9.2.3.

ADDITIONAL "TUNING" OF SYSTEM

San Juan and Miami have reasonably reliable long-term records of winds associated with tropical cyclones. These records suggest that the simulations slightly over-estimated the return periods at both sites for winds below hurricane force. To correct for this tendency, the frictional factor, by trial and error, was slightly adjusted to effectively, "tune" the system. It is considered likely that additional minor modifications, similar to the above, will periodically be made to the algorithm as additional research is conducted on this topic and after the program is run for a larger sample of sites.

CONFIDENCE FACTORS

In connection with statistical forecasting, the question often arises as to the confidence of the projections. Confidence limits generally refer to a specific step in a procedure and, because of the multiplicity of steps, a quantified estimate would be difficult to obtain. However, much can be said about the results in the qualitative sense.

Batts et al. (1980) point out that there are four principal sources of error in procedures of this type: (1) sampling errors, due to the limi-

ted size of the data sample used in making the statistical inferences (currently, 102 years); (2) probabilistic modeling errors due to the imperfect choice of the distribution functions to which the climatological data are fitted (i.e., assuming a log-normal distribution of RMW when a normal could, perhaps, have been more appropriate); (3) observation errors, due to the imperfect measurement or recording of the true values of the various parameters and; (4) physical modeling errors, due to the imperfect representation of the dependence of the wind speed upon the various climatological characteristics and micrometeorological parameters.

The authors in the above cited reference provide a rather thorough assessment of these four sources of error and the reader is referred to their study for details. To their evaluation could be added the problem of mixed frequency distributions. In examining the Weibull fit to wind distributions from various sites throughout the tropical cyclone basin, a mixture problem (Crutcher and Joiner, 1977) was sometimes apparent. The proper way to handle these mixtures would be to separate the data into its components, treat each component separately and then sum the individual probabilities. Although an initial attempt was made to do this in HURISK, this was abandoned when it became apparent that such a procedure would add an enormous degree of subjectivity to an otherwise entirely objective procedure. In that the HURISK algorithm does provide (through Chart 8) a plot of the Weibull fit to the data, the problem, when it occurs, is quite apparent. In view of this, not formally addressing the mixture problem was considered an acceptable tradeoff.

Many of the same type of sensitivity tests discussed in Batts et al. were conducted on HURISK. The general impression obtained from these latter tests was that there are many assumptions, approximations, distributions, procedures, etc. which do, indeed, effect the outcome but each in a rather small (0 to 5% variation) way. If these effects were additive, a sizeable error could result. If, on the other hand, the errors tend to cancel, then the net error would be small. In actual fact, something between these two extremes is probably realistic. It was definitely noted in all the sensitivity tests, that the largest differences were on the extended return periods, (beyond 100-year events).

Thus, without a large amount of additional simulation using all possible combinations of parameters which contribute to the outcome, a specific quantitative assessment of confidence in the various return periods, cannot be made. One would have to question the value of these confidence factors since they would probably be quite broad particularly for the extended return periods. It suffices to say that the estimates presented are the best that can be attained using the available data and computer resources coupled with a reasonable amount of statistical and meteorological insight.

REFERENCES

- Abernethy, R.B., J.E. Breneman, C.H. Medlin, and G.L. Reinman, 1983: Weibull Analysis Handbook. AFWAL-TR-83-2079, USAF, Aero Propulsion Laboratory, Wright-Patterson AFB, 228 pp.
- Akima, H., 1970: A new method of interpolation and smooth curve fitting based on local procedures. J. Assoc. Computing Mach., 17, 589-602.
- Akima, H., 1986: A Method of Univariate Interpolation That Has the Accuracy of a Third-degree Polynomial. NTIA Report Series 86-208, Boulder, CO., 69 pp.
- ANSI (American National Standards Institute), 1982: American Standard Minimum Design Loads for Buildings and other Structures. ANSI A58.1-1982, New York, NY, 100 pp.
- Batts, M.E., M.R. Cordes, L.R. Russell, J.R. Shaver and E. Simiu, 1980: Hurricane Wind Speeds in the United States. NBS Building Science Series 124. (National Bureau of Standards), 41pp.
- Burington, R.S. and D.C. May, 1958: Handbook of Probability and Statistics. Handbook Publishers, Inc., Sandusky, Ohio, 332 pp.
- Crutcher, H.L., and R.G. Quayle, 1974: Mariners Worldwide Guide to Tropical Storms at Sea. NAVAIR Atlas 50-1C-61, Washington, D.C., 424 pp.
- Crutcher, H.L. and R.L. Joiner, 1977: Separation of Mixed Data Sets into Homogeneous Sets. NOAA Technical Report EDIS 19, Asheville, NC, 167 pp.
- Crutcher, H.L. and R.L. Joiner, 1978: Gamma Distribution Bias and Confidence Limits. NOAA Technical Report EDIS 30, Rockville, MD, 46 pp. plus Appendices.
- Crutcher, H.L. and R.L. Joiner, 1980: Gamma Distribution Shape Parameter Bias. NOAA Technical Memorandum EDIS 29, Washington, D.C., 38 pp.
- Emanuel, K.A., 1986: An air-sea interaction theory for tropical cyclones. Part I: Steady-state maintenance. J. Atmos. Sci., 30, 585-604.
- Georgiou, P.N., A.G. Davenport and B.J. Vickery, 1983: Design wind speeds in regions dominated by tropical cyclones. Proceedings, 6th International Conference on Wind Engineering, Gold Coast, Australia and Auckland, N.Z. (Elsevier Science Publishers B.V.)
- Georgiou, P.N., 1985: Design Wind Speeds in Tropical Cyclone Prone Regions. University of Western Ontario Research Report BLWT-2-1985, London, Ontario, Canada, 295 pp.

- Hahn, G.J. and S.S. Shapiro, 1967: Statistical Models in Engineering. John Wiley and Sons, New York, NY, 354 pp.
- Hamming, R.W., 1962: Numerical Methods for Scientists and Engineers. McGraw-Hill Book Company, Inc., New York, NY, 411 pp.
- Ho, F.P., 1975: Storm Tide Frequency Analysis for the Coast of Puerto Rico. NOAA Technical Memorandum NWS HYDRO-23, Silver Spring, MD, 41 pp.
- Ho, F.P., J.C. Su, K.L. Hanevich, R.J. Smith and F.P. Richards, 1987: Hurricane climatology for the Atlantic and Gulf Coasts of the United States. NOAA Technical Report NWS 38, National Weather Service, Silver Spring, MD, 195 pp.
- Hope, J.R. and C.J. Neumann, 1968: Probability of Tropical Cyclone Induced winds at Cape Kennedy. ESSA Technical Memorandum WBTM SOS-1, Silver Spring, MD, 67 pp.
- Hope, J.R. and C.J. Neumann, 1970: An operational technique for relating the movement of existing tropical cyclones to past tracks. Mon. Wea. Rev., Vol. 98, No. 12, 925-933.
- Hope, J.R. and C.J. Neumann, 1971: Computer methods applied to Atlantic area tropical storm and hurricane climatology. Mar. Wea. Log, Vol. 15, No. 5 (Sept., 1971), 272-278.
- Jarvinen, B.R., C.J. Neumann and M.A.S. Davis, 1984: A Tropical Cyclone Data Tape for the North Atlantic Basin, 1886-1963: Contents, Limitations, and Uses. NOAA Technical Memorandum NWS NHC 22, National Hurricane Center, 21 pp.
- Jarvinen, B.R. and A. Barry Damiano, 1985: A Storm Surge Atlas for Corpus Christi, Texas. NOAA Technical Memorandum NWS NHC 27, National Hurricane Center, 518 pp.
- Merrill, R.T., 1982: A Comparison of Large and Small Tropical Cyclones Atmospheric Science Paper No. 352, Colorado State University, Fort Collins, CO, 75 pp.
- Mills, F.C., 1955: Statistical Methods. Holt, Rinehart and Winston, New York, NY, 842 pp.
- Myers, V.A., 1954: Characteristics of United States Hurricanes Pertinent to Levee Design for Lake Okeechobee, Florida. Hydrometeorological Report No. 32, U.S. Weather Bureau, Department of Commerce and U.S. Army Corps of Engineers, Washington, D.C., 108 pp.
- Neumann, C.J., 1969: Probability of Tropical Cyclone Induced Winds at NASA Manned Spacecraft Center. ESSA Technical Memorandum WBTM SOS 4, Silver Spring, Md., 46 pp.
- Neumann, C.J., 1972: An Alternate to the HURRAN Tropical Cyclone Forecast System. NOAA Technical Memorandum NWS SR-63, Fort Worth, TX, 32 pp.

- Neumann, C.J., 1985: On the calculation of tropical cyclone return periods. Extended Abstracts Volume, 16th Conf. on Hurricanes and Tropical Meteorology, American Meteorological Society, Boston, MA, 176-177.
- Neumann, C.J., B.R. Jarvinen, A.C. Pike and J.D. Elms, 1987: Tropical Cyclones of the North Atlantic Ocean, 1871-1986. Historical Climatology Series 6-2, National Climatic Data Center and National Hurricane Center, 186 pp.
- Neumann, C.J. and M.J. Pryslak, 1981: Frequency and Motion of Atlantic Tropical Cyclones. NOAA Technical Report NWS 26, Washington, D.C., 64 pp.
- Russell, L.R., 1971: Probability distributions for hurricane effects. Journal of the Waterways, Harbors and Coastal Engineering Division. ASCE, Vol. 97, No. WW1 (Feb., 1981), 139-154.
- Schwerdt, R.W., F.P. Ho and R.R. Watkins, 1979: Meteorological Criteria for Standard Project Hurricane and Probable Maximum Hurricane Windfields, Gulf and East Coasts of the United States. NOAA Technical Report NWS 23, National Weather Service, Silver Spring, MD, 317 pp.
- Shea, D.J. and W.M. Gray, 1973: The hurricane's inner core region I: Symmetric and asymmetric structure, J. Atmos. Sci., 30, 1544-1564.
- Sheets, R.C., 1972: Some statistical characteristics of the hurricane eye and minimum sea-level pressure. Annual Report, 1971, Project Stormfury, Miami, FL, 143-156.
- Shuman, F.G., 1957: Numerical methods in weather prediction, II: Smoothing and filtering. Mon. Wea. Rev., Vol. 85, 357-361.
- Simiu, E. and R.H. Scanlan, 1978: Wind Effects on Structures. Wiley-Interscience, New York, NY, 458 pp.
- Tsokos, C.P., 1972: Probability Distributions: An Introduction to Probability Theory with Applications. Duxbury Press, Belmont, CA, 657 pp.
- Willoughby, H.E., J.A. Clos and M.G. Shoreibah, 1982: Concentric eye walls, secondary wind maxima, and the evolution of the hurricane vortex. Journ. Atmos. Sci., Vol. 39, No. 2 (Feb. 1982), 395-411.
- Xue, Z. and Charles J. Neumann, 1984: Frequency and motion of Western North Pacific tropical cyclones. NOAA Technical Memorandum NWS NHC 23, National Hurricane Center, 89 pp.